CALCIUM-DEPENDENT GLOBAL CHROMATIN COMPACTION PROTECTS DNA FROM UV INFLICTED DAMAGE

A DISSERTATION

SUBMITTED IN PARTIAL FULFILLMENT OF THE REQUIREMENTS

FOR THE DEGREE OF DOCTOR OF PHILOSOPHY

IN THE GRADUATE SCHOOL OF THE

TEXAS WOMAN'S UNIVERSITY

DEPARTMENT OF BIOLOGY

COLLEGE OF ARTS AND SCIENCES

BY

Mohammad M. Abbas, M.S.

DENTON, TEXAS

December 2019

Dedication

For my loving wife, Manar Alsayyed, my always encouraging wife, to my smart kid Faris Abbas (Abu Hamza) and my beautiful daughters Talia Abbas, Aleena Abbas, and Tima Abbas.

Acknowledgments

First and foremost, I would like to express my sincerest gratitude to my advisor Dr. Michael Bergel for giving me the opportunity to work on this project and his continual guidance and advice in every aspect of my research, and for being patiently by my side during these years. Without his constructive feedback and continuous encouragement, I would not have been able to complete the dissertation.

I am incredibly grateful to all of my committee members Dr. Heather Conrad-Webb, Dr. Camelia Maier, Dr. Nathanial C. Mills, and Dr. Rebecca Dickstein, for their valuable suggestions, feedbacks in evaluating my research.

I would like to thank Dr. Claire L. Sahlin and the Biology Department Chair Dr. Juliet V. Spencer, for their kindness and support.

A big thanks to all the members of our laboratory, Dr. Mangalam Subramanian, Dr. Rhiannon W. Gonzalez, Dr. LaTandra J. Lawrence, Dr. Suhdeer Dhanireddy, Dr. Carrie Wilks, Mr. Amon Gekombe, Mr. Christopher Buliga, Ms. Christina Rohmer, and Rituparna Sinha Roy, It was a pleasure to work with such a wonderful group.

Finally, I must express my gratitude to my mother, who took care of me as a child and supported me as a grown-up man. She blindly supported me during this long journey, giving me strength and confidence to believe in myself in every situation I encountered. I would also like to thank my brothers and sisters for their continuous support, this work could not have been done without their encouragement.

LIST OF ABBERVIATIONS

6-4PPs - Pyrimidine (6-4) Pyrimidone Photo Products

Ac - Acetyl

ACF -ATP- Dependent Chromatin Remodeling Factor 9

Ac-H3K9 - Acetylated Histone H3 lysine 9

ANOVA - Analysis of Variance

ANT – Adenine Nucleotide Translocator

APO-1 – Apoptosis Antigen 1

APAF-1 – Apoptotic Protease Factor 1

ARR – Acess Repair Restore

BER – Base Excision Eepair

CO_2 – Carbon Dioxide

CPDs - Cyclobutane Pyrimidine Dimers

CS - Cockyane Syndrome

CFP - Cyan Flurescent Protein

DAP I- 4′,6-Diamidino-2-Phenylindole

DDB1/2 - Damaged DNA Binding Complex 1 and 2

DMSO - Dimethylsulfoxide

DNA - Deoxyribonucleic Acid

DSB - Double Strand Break Repair

EDTA – Ethylene Diamine Tetraacetic Acid

EGTA – Ethylene Glycol Tetraacetic Acid

ER – Endoplasmic Rericulum

ERCC1 - Excision Repair Cross Complementing Protein 1

FITC - Fluorescein Isothiocyanate

GFP - Green Fluorescent Protein

GGR - Global Genome Repair

H1 - Linker Histone

H2/H3/H4 - Core Histones

H3k14 - Histone H3 Lysine 14

H3K14 - Histone H3 Lysine 9

H4K5 - Histone H4 Lysine 5

HAT - Histone Acetyltransferase

HCT116 – Colon Cancer Cell line 116

HDAC - Histone Deacetylase

HDACis - Histone Deacetylase inhibitors

HMG – High mobility Group Proteins

Hp1 – Heterochromatin Protein

HHR – Homologous Recombination

HYBOND N+ - Positively Charged Nylon Membrane

LacR – Lactose operon repressor

LacO – Lactose operon operator

MEF-Embryonic Fibroblast

MNase - Micrococcal Nuclease

NCS - Neocarzinostatin

NER- Nucleotide Excision Repair

NHEJ - Non-Homologous End Joining

N- terminal - Amino Terminal

PAGE - Polyacrylamide Gel Electrophoresis

PBS - Phosphate Buffer Saline

PMST – Phenylmethylsulfonyl Fluoride

PTM - Post Translation Modification

Rec - Recombinant

RIPA- Radio Immunoprecipitation Assay

RNA-POI II - Ribonucleic Acid Polymerase II

RFC – Replication Factor C

ROS – Reactive Oxygen Species

SD - Standard Deviation

SDS – Sodium Dodecyle Sulfate

SE - Standard Error

SWI- Switching (Yeast)

TEA – Tris-EDTA Acetate Buffer

TCR - Transcription Couple Repair

TRPA1 – Transient Receptor Potential A1

TSA -Trichostatin A

TNF – Tumor Necrosis Factor

TTD - Trichothiodystrophy

UV - Ultra Violet

UVA - Ultraviolet Subtype A

UVB - Ultraviolet Subtype B

UVC - Ultraviolet Subtype C

VDSC – Voltage-Dependent Anion Channel

WB - Western Blot

XP - Xeroderma Pigmentosum

ABSTRACT

CALCIUM-DEPENDENT GLOBAL CHROMATIN COMPACTION PROTECTS DNA FROM UV INFLICTED DAMAGE

MOHAMMAD M. ABBAS

DECEMBER 2019

Eukaryotic genomes are packaged into chromatin, which is the physiological substrate for all DNA-mediated functions, including DNA damage repair. At the DNA damage site, chromatin organization undergoes critical rearrangements during the repair process. These rearrangements around the lesion sites accommodate at least three steps: providing access to the repair factors, repair, and restoring the DNA's pre-lesion chromatin architecture. However, the global changes to chromatin after UV-irradiation were less explored and understood. To investigate the relationship between chromatin condensation and UV irradiation, HeLa-S3 cells were irradiated and subjected to micrococcal nuclease digestion analysis. The results showed that chromatin globally commenced compaction five minutes after UV-irradiation. Twenty-four hours after irradiation chromatin returned to the pre-UV steady-state. Southwestern blots showed that cells were irradiated twice at 15 J/m^2 with a five minutes break had a significantly lower cyclobutane pyrimidine dimers (CPD) and DNA (6-4) photoproduct (6-4PP) rate in comparison to cells subjected to 30 J/m^2, and had no significant difference from cells irradiated with a single dose of 15 J/m^2. Western blot analysis demonstrated a post-UV core histone deacetylation wave, that followed the chromatin condensation. Western blots analysis of caspase-3, which is activated in apoptotic cells both by

extrinsic and intrinsic pathways, showed no caspase-3 activation after five and ten minutes post UV-irradiation. Here, we demonstrate that an environmental genotoxic agent, UV radiation, causes immediate and global chromatin compaction in HeLa cells and this compaction results in a robust reduction in the newly formed lesions. Our data suggest an influx of calcium cations after UV irradiation is directly involved in inducing chromatin compaction.

TABLE OF CONTENTS

LIST OF FIGURES

CHAPTER I

Introduction

Chromatin Structure

The basic unit of chromatin the nucleosome, is made up of four core histones – H2A, H2B, H3, and H4 – each in duplicate (Kornberg and Thomas, 1974; Smith and Workman, 2012). Together they organize 146 base-pairs (bp) of DNA that wraps 1.65 times in a left-handed wrap around the histone octamer (Luger et al., 1997). These proteins are highly conserved across eukaryotes, are low in molecular weight, and contain a central histone fold domain mediates histone-histone and histone-DNA interactions. Each histone also possesses unstructured short N-terminal – and sometimes C-terminal as well – domains, often referred to as histone "tails," that extend out from the nucleosome core (Carruthers and Hansen, 2000). Even though these tails are not required for nucleosome core particle assembly, they do function in higher order folding of the chromatin fiber (Horn and Peterson, 2002). In addition, the tails contain a multitude of sites for post-translational modifications (PTMs) that are key in regulating multiple biological functions (Peterson and Laniel, 2004; Rando and Winston, 2012). The primary structure of chromatin is the "beads on a string" structure, which represents single nucleosomes in a linear formation as seen by cryo-electron microscopy (Woodcock, 2006). This 10-12 nm thick fiber is then folded into the more common three-dimensional structure termed the 30 nm fiber through inter-nucleosomal interactions. This structure is further stabilized by the addition of a fifth class of histone, the linker histone H1 (Robinson and Rhodes, 2006). Linker histones bind nucleosomes at the

entry-exit point at a one-to-one ratio and stabilize an additional 20-60 bp of linker DNA (Woodcock et al., 2006). The 30 nm fibers can then self-associate into even larger 100-400 nm thick structures called chromonema filaments. These structures predominate in the nucleus even during interphase when the need to access DNA is high. Further folding of chromatin form the highest-order structure which is the mitotic/meiotic chromosome in which the DNA is compacted some 700 nm fold relatively to the 2 nm DNA duplex (figure 1) (Woodcock and Ghosh, 2010).

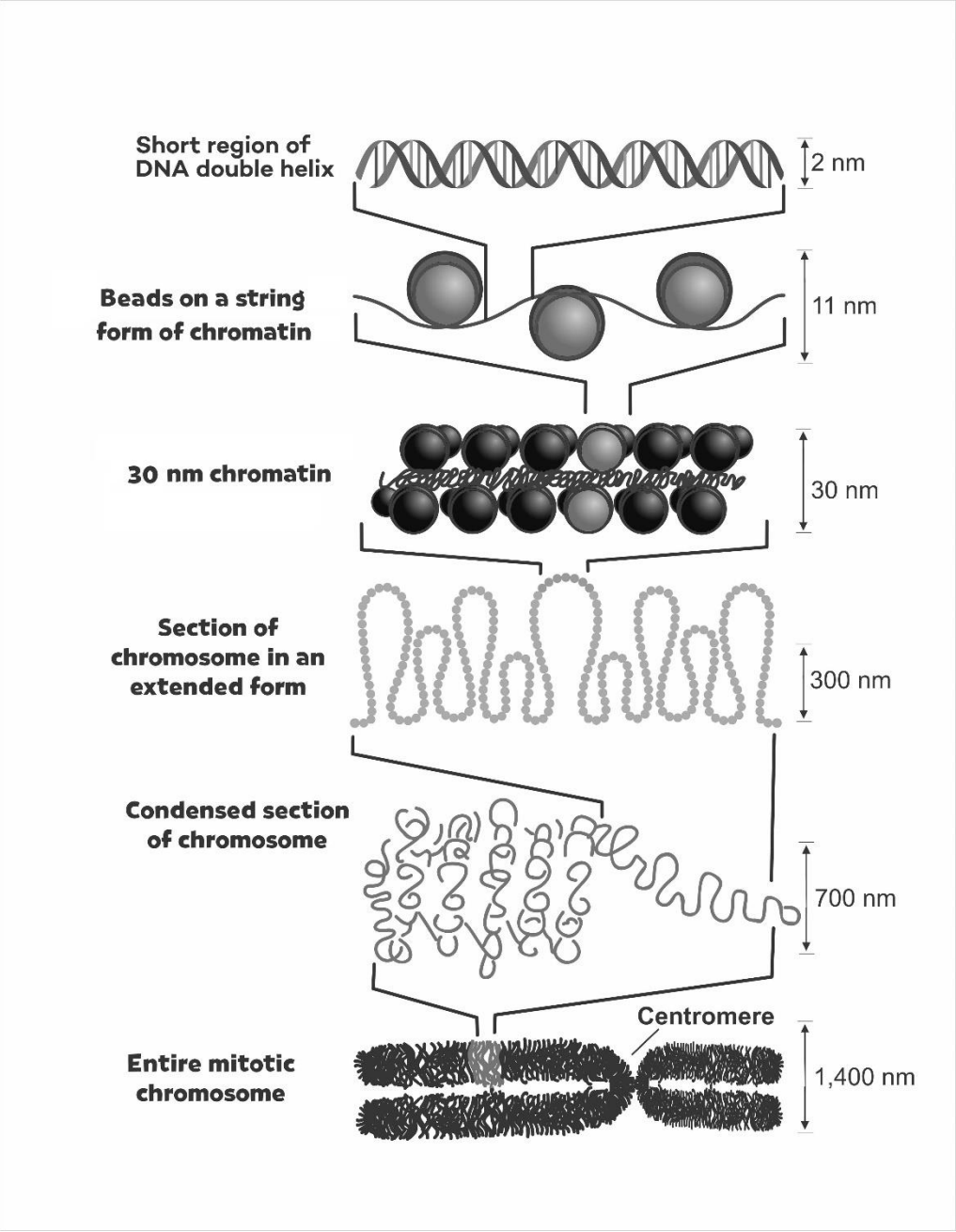

Figure 1. Levels of Chromatin structure and compaction in the human genome. The compaction of DNA into chromatin from 2 nm fiber to 1400 nm mitotic/meiotic chromosomes, adapted from: Felsenfeld and Groudine, 2003 .

Euchromatin *versus* Heterochromatin

Chromatin has been subdivided into two functional classes; euchromatin and heterochromatin (figure 2), both refer to a state of compaction and transcriptional potentials. Euchromatin a form of chromatin is decondensed in the interphase of cell cycle and contains most of actively transcribed genes. Heterochromatin initially, before the discovery the structure of DNA was defined as the region of nuclei that stained strongly with basic dyes. Heterochromatin tends to be located at the nuclei periphery, where it has specific interaction with nuclear envelope, and forms blocks surrounding the nucleolus. Heterochromatin remains condensed throughout the cell cycle and contains mostly inactive genes (Passarge, 1979). Today, the term heterochromatin is broadly applied and is often extended to include the transcriptionally silent regions of chromatin, disregarding their staining properties. Heterochromatin also has been subdivided into classes: facultative heterochromatin and constitutive heterochromatin. The latter is permanently compact, and abundant in repetitive, gene poor, and late replicating DNA sequences, while the facultative heterochromatin can reversibly undergo transition from a close, transcriptionally inefficient state to become more open, and transcriptionally adequate (Trojer and Reinberg, 2007).

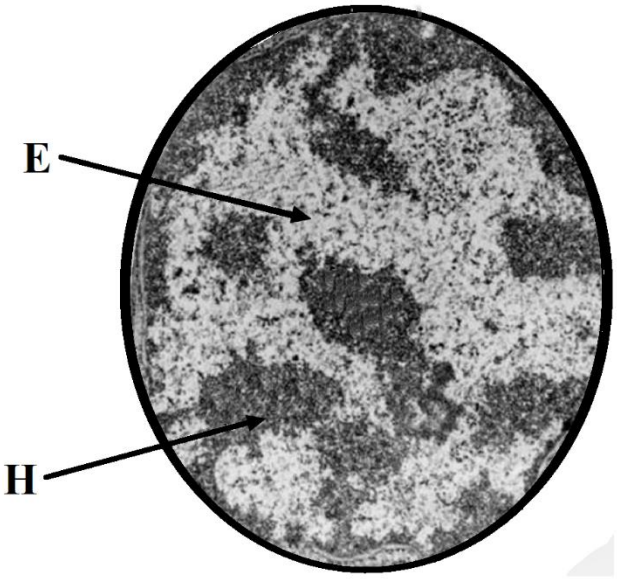

Figure 2. Euchromatin (E) and heterochromatin (H) in an interphase nucleus adapted from: (Wang et al., 2014)

Chromatin Response to Stress

Chromatin is not simply a packaging tool, it's also dynamically modified in ways that reflect the regulatory cues necessary to program appropriate cellular pathways. Recent studies revealed the importance of chromatin's role in stressed versus non-stressed conditions. Specific chromatin domains have different responses under different stresses (Smith and Workman, 2012). The dynamic state of chromatin can be influenced by cellular and environmental agents, which trigger the conformational changes that make the chromatin more open. For instance unwrapping transiently exposes buried DNA sites for access to repair machinery factors and proteins. Any process that entails access to DNA must conquer this chromatin structural natural suppressive barriers (Kornberg and Lorch, 1999b). In stressed situations chromatin modifiers can overcome the chromatin natural barriers, and these modifiers to three main groups: (1) ATP- dependent chromatin remodelers machines such as the SWI/SNF-superfamily of DNA-dependent ATPases (Loyola and Almouzni, 2007; Neves-Costa and Varga-Weisz, 2006) that alter chromatin structure, making the DNA accessible to the proteins which bind chromatin and regulate cellular processes; (2) Histone modifying complexes which influence the epigenetic modifications of various histones by altering the N-terminal tails of chromatin, and therefore the overall dynamic state of chromatin (Chakravarthy et al., 2005; He and Lehming, 2003); (3) Differential binding of abundant non-core histone proteins, such as the linker histone H1, the family of high mobility group proteins (HMG), or different isoforms of the hetero-chromatin protein 1 (HP1).

These chromatin modifiers are significant in the link between chromatin structure and cellular processes such as cell cycle control, replication, recombination, transcription, aging, and death signaling. Chromatin modifiers also respond to external stimuli or stresses such as hypoxia, ionizing radiation, ultraviolet radiation (UV), oxidative stress, endoplasmic reticulum (ER) stress, heat shock, toxicants, hyperosmotic stress, and nutrient and starvation stress (Pecinka and Mittelsten Scheid, 2012).

UV-Induced Damage and Cellular Response

Ultraviolet radiation (UVR) is an electromagnetic radiation whose wavelength lies between that of visible light and X-rays in the electromagnetic spectrum. It is divided into three different ranges of wavelengths: ultraviolet A (UVA, 315–400 nm), ultraviolet B (UVB, 280–315 nm), and ultraviolet C (UVC, 100–280 nm) (Anna et al., 2007; Slominski and Pawelek, 1998). UVC is considered as the most harmful radiation and produce the maximal DNA damage. However, it does not reach to the Earth’s surface as it is absorbed via the stratospheric ozone layer, although exposure to UVC might happen through manmade sources, like germicidal lamps. Around 95% of UVA and 5% of UVB reach the earth's surface and this has important biological consequences for the skin and eyes of humans. The extent of UV rays reaching the Earth's surface depends on a number of factors like the time of day, and the time of year; its intensity is strongest during summer and at early afternoon. Latitude and altitude might play a role in the UVR level; UVR intensity increases at places close to the equator and at higher altitudes.

UV radiation leads to the formation of several types of dimeric lesions, including cyclobutane pyrimidine dimers (CPD) and 6-4 photoproducts (6-4PP) (Douki, 2006) (figure 3), Both of these lesions distort DNA's structure, introducing bends or kinks and thereby impeding DNA transcription and replication, therefore causing genomic instability (Friedberg, 2003). If they are not repaired before the cell cycle S phase, they can result in an incorporation of incorrect nucleotide, or mutations being integrated into newly synthesized DNA. In addition, UV causes oxidative damage that form 8-oxo-deoxyguanine (8-oxo-dG) lesions (Dahle and Kvam, 2003).

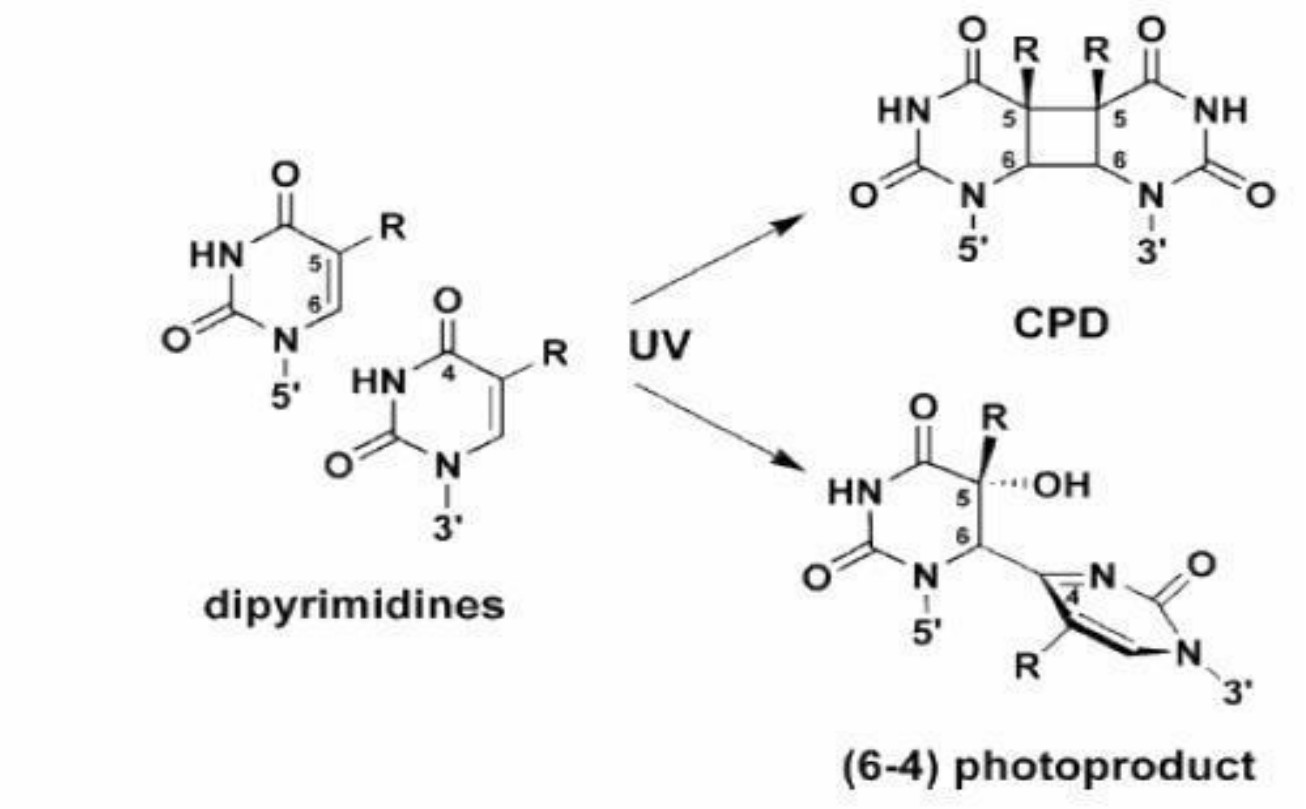

Figure 3: Absorption of UV light can result in two main lesions between adjacent pyrimidines. These are cyclobutane pyrimidine dimers (CPD), which predominantly form between two thymines by the formation of a four-membered ring by the saturation of the double bonds between C5 and C6 of two adjacent pyrimidines. Also, (6-4) photoproducts are formed between C4 position and C6 position of two adjacent pyrimidines, most frequently T-C sites. This figure is adapted from: (Douki, 2013).

UV Damage Repair by Nucleotide Excision Repair

To maintain the genetic homeostasis by counterbalancing these photolesions, nucleotide excision repair (NER) pathway is involved in removing such lesions in eukaryotes and prokaryotes or the cells undergo apoptosis when the burden of the genetic damage is beyond repair (Huen and Chen, 2010). Upon UV radiation, cells are arrested in G1 and G2 phases of the cell cycle, both of which are regulated by tumor suppressor p53 (Decraene et al., 2001). In eukaryotes, the NER pathway is subdivided into two pathways: global genome repair (GGR) which repairs photolesions located anywhere within chromatin, and transcription coupled repair (TCR), which efficiently removes lesions in the transcriptionally active genes (Lin and Wilson, 2007).

In TCR, the damage sensing and initiation of repair carried out by cockayne syndrome group A (CSA) and cockayne syndrome group B (CSB) that recognize stalled elongated RNA polymerase II (RNAP2). ATP-dependent chromatin remolding protein CSB and the WD40 domains (also known as WD, which is one of the most abundant domains and also among the top interacting domains in eukaryotic genomes) containing Cockayne Syndrome protein A also have very important roles in the photolesions site recognition and repair (Henning et al., 1995). Global genome repair (GGR) is carried out by DNA damage binding protein 1 and 2 (DDB1-DDB2) and the xeroderma pigmentosum group C protein complex XPC-HR23B (XPC-HR23B centrin-2). The DDB1-DDB2 complex has the highest known affinity for photodimers in metazoan cells, and serves in the initial detection of UV-lesions *in vivo* (Scrima et al., 2008). This complex recruits XPC-HR23B centrin-2 to photolesion regions (Palomera-Sanchez and Zurita, 2011). The DDB1-DDB2 complex localizes to chromatin following UV-irradiation and remains tightly

attached to mononucleosomes when chromatin is solubilized by micrococcal nuclease digestion (Groisman et al., 2003).

The following steps of TCR and GGR merge into a common mechanism in which the transcriptional factor II (TFIIH) is recruited (Volker et al., 2001). The bidirectional helicase of TFIIH opens the damaged DNA sequence over a stretch of around 30 nucleotides (Fuss and Tainer, 2011). The unwound DNA is stabilized by DNA repair protein complementing XP-A (XPA), Replication protein A (RPA), and DNA repair protein complementing XP-G (XPG) which are considered the pre-incision complex which is assembled around the damage site (Oksenych and Coin, 2010). XPA with the single strand DNA binding complex RPA act as an organizational factor, so that the repair machinery is positioned around the lesion. XPA and RPA are believed to protect the undamaged strand and lead to complete opening of the damaged DNA (Andressoo et al., 2006). Additionally, RPA interacts with several other factors like the endonuclease XPG. The DNA excision repair protein ERCC-1 and DNA repair protein complementing XP-F (ERCC1-XPF) dimer facilitates the correct positioning of the endonucleases and incises the damage site at 5` position relatively to the lesions and XPG incises the DNA 3` ends from the lesion. The result is 25-30 nucleotide single strand gap that is filled by DNA replication with the involvement of the proteins: Proliferating cell nuclear antigen (PCNA), RPA, and the polymerase activity of ε, δ (Ogi et al., 2010). Eventually replication factor C (RFC) and or ERCC1 recruit DNA ligase to ligate the nick (figure 4).

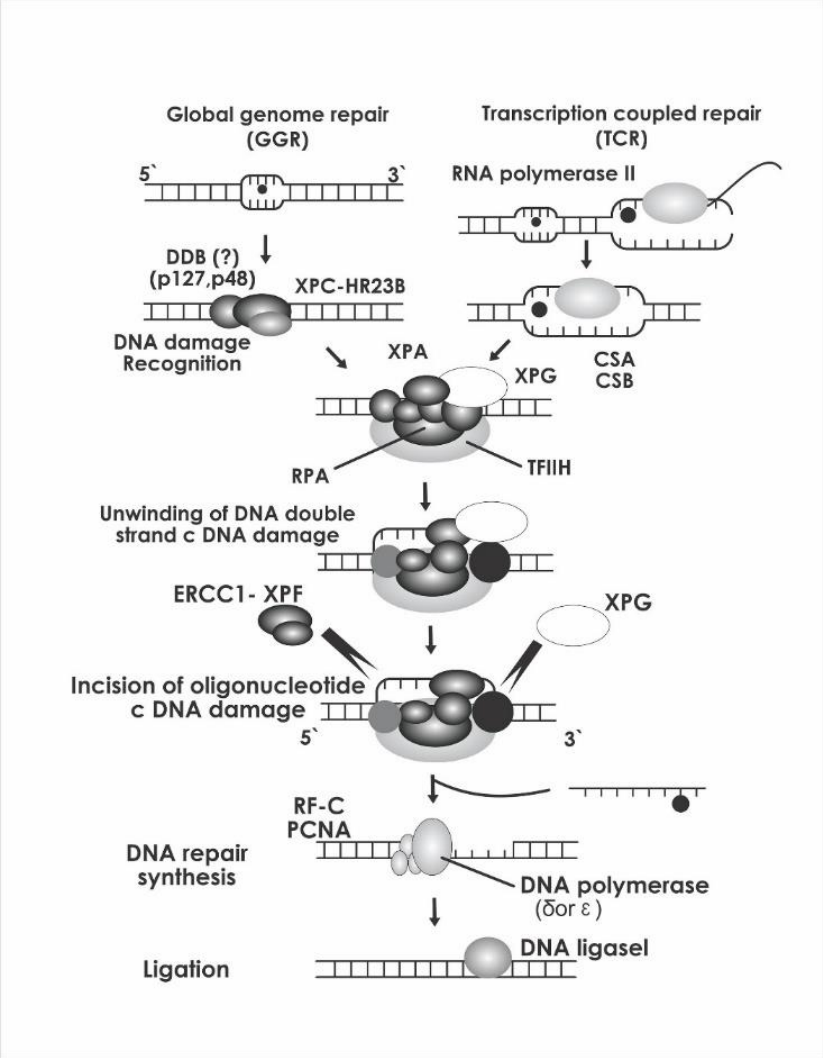

Figure 4. Nucleotide excision repair (NER) mechanism in eukaryotes. There are two routes for the repair of DNA photolesions: global genome repair (GG-NER) and transcription coupled repair (TC-NER). In first route, the damaged sites are recognized by the complex protein XPC-hHR23B. In the second route, TC-NER is initiated by the arrest of RNA polymerase II at a lesion on the transcribed DNA strands. Following recognition, the DNA lesions are unwind by activation of transcription factor IIH (TFIIH), and then replication protein A binds the single-stranded DNA. The damage is cleaved on both the 3' and 5' sites, which releases the damaged DNA fragment. Gap filling proceeds by DNA replication factors such as replication factor C (RF-C) and DNA polymerase δ/or ε, using the opposite DNA strand as a template. Finally, the new synthesized DNA is ligated by DNA ligase adapted from: (Ichihashi et al., 2003)

Programmed Cell Death (Apoptosis)

Apoptosis is the best-characterized type of programmed cell death, and it is essential in development and homeostasis and in pathogenesis of different diseases such as cancer. If the level of damaged DNA damage arising from oxidation stress, UV radiation, ionizing radiation, or other stresses that are beyond repair, the cell will be removed by apoptosis (Wong, 2011). Extensive lesions in DNA will cause blockage in DNA replication, leading to collapse of replication forks and this will induce apoptosis. Some of the first event of apoptosis include shrinkage and chromatin condensation that degrade and separates into individual bodies called apoptotic bodies (figure 5). Consequently, the apoptotic cells are engulfed by macrophages and dendritic cells (Fullgrabe et al., 2010).

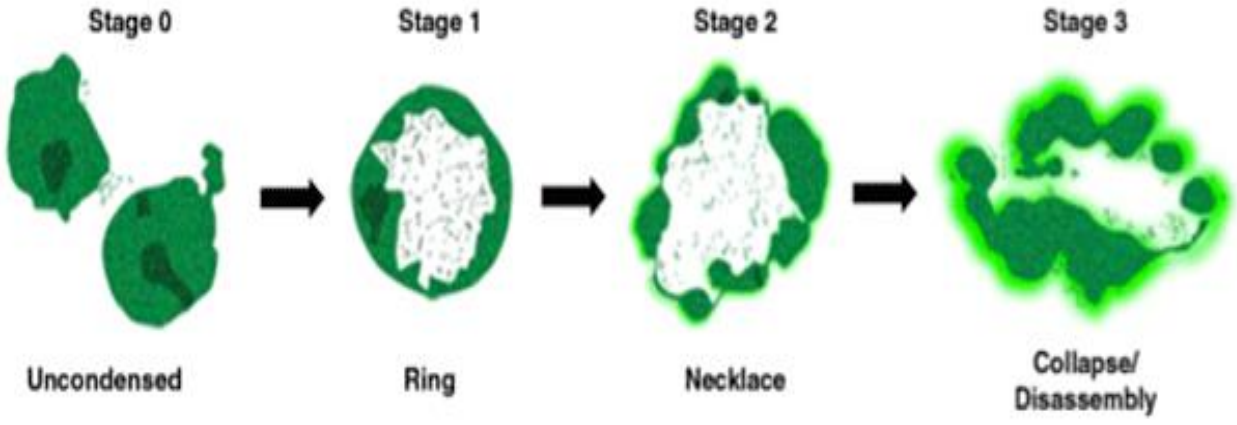

Figure 5. Shown is the process of chromatin condensation and shrinkage during apoptosis. Adapted from: Nuclear-ID chromatin condensation kit by Enzo.

Apoptosis is initiated by two major pathways in mammalian cells, depending whether the stimulating factor is extrinsic, or intrinsic. However, there is now evidence that the two pathways are linked and that molecules in one pathway can influence the other (Igney and Krammer, 2002). The extrinsic pathway is triggered through specific cell surface death receptors such as tumor necrosis factor-α (TNF) and apoptosis antigen 1 (APO-1 or APT) also known as Fas receptor.

Many stresses that cause chromatin and DNA damage such as cytotoxic drugs activate intrinsic pathway of apoptosis that begins with the permeabilization of the mitochondrial outer membrane. The mechanisms through which this occurs remain controversial, however, it is thought that permeabilization can be either permeability transition (PT) pore dependent or independent (Green and Kroemer, 2004). The PT pore is comprised of the matrix protein cyclophilin D, the inner mitochondrial membrane protein adenine nucleotide translocator (ANT), and the outer mitochondrial membrane protein voltage-dependent anion channel (VDAC) (Crompton et al., 1998). The opening of the PT pore triggers the dissipation of the proton gradient created by electron transport, causing the uncoupling of oxidative phosphorylation. The opening of the PT pore also causes water to enter the mitochondrial matrix, which results in swelling of the intermembranal space and rupturing of the outer membrane causing the release of apoptogenic proteins (Yang and Cortopassi, 1998). Cytochrome c and another factor called apoptotic protease activating factor 1 (APAF-1) form a large oligosome complex termed as apoptosome.

This leads to posttranslational modification at specific residues of p53, resulting in activation of downstream genes including cyclin-dependent kinase inhibitor 1 (*p21)*, growth arrest and DNA-damage-inducible protein GADD45 alpha (*GADD45a*), and the murine double minute 2 (*MDM2*), which leads to the recruitment of the caspases enzymes that carry out the cell death (Danial and Korsmeyer, 2004).

Physiological Protective Mechanisms Against DNA Damage Induced by Radiation

Many known molecular and physiological responses are initiated upon UV radiation. One of these physiological responses is the signaling pathway that leads to hyperpigmentation in the human melanocytes (Miyamura et al., 2007; Moan et al., 2012). The skin covers the whole-body surface and acts as a dynamic barrier to prevent water evaporation from the human body. It also prevents the entrance of toxic and harmful substances and pathogens into vital internal organs. However, the integrity of skin barriers can be impaired by exogenous factors, including ultraviolet rays (UVR). Anatomically, skin is divided into epidermis, dermis, and subcutaneous tissue. Epidermis can be further divided into several layers, which include from the deepest basal layer, spinous layer, granular layer, and cornified layer, depending on the differentiation level of the keratinocytes, the major cell type in the epidermis (figure 6A) (Pincelli and Marconi, 2010). In addition to keratinocytes, the main cells in the epidermis include melanocytes and Langerhans cells (LCs). Most of the melanocytes are distributed in the basal layer, synthesizing and transferring melanin to adjacent keratinocytes, and contributing to skin color and photoprotection (figure 6B) (Gray-

Schopfer et al., 2007). Human skin detects the UV component of the sunlight through a photoreceptor rhodopsin, which is also expressed in melanocytes (Wicks et al., 2011). The signaling pathway that senses UV by rhodopsin induces calcium influx in melanocytes via the ion channel transient receptor potential A1 (TRPA1) and activation of phosphodiesterase C, which leads to early melanin synthesis and redistribution to protect cells layers beneath the melanocytes (Bellono et al., 2013). This mode of DNA protection is a long-term mechanism that begins several hours to days after UV exposure (Beattie et al., 2005; Park et al., 2002). Failure to produce melanin, for example, due to the loss of function of tyrosinase as in ocular cutaneous albinism type 1, leads to accumulation of UV radiation-induced DNA damage that results in a dramatically increased risk for squamous and basal cell carcinoma as well as malignant melanoma (Bivik et al., 2006; Bohm et al., 2005).

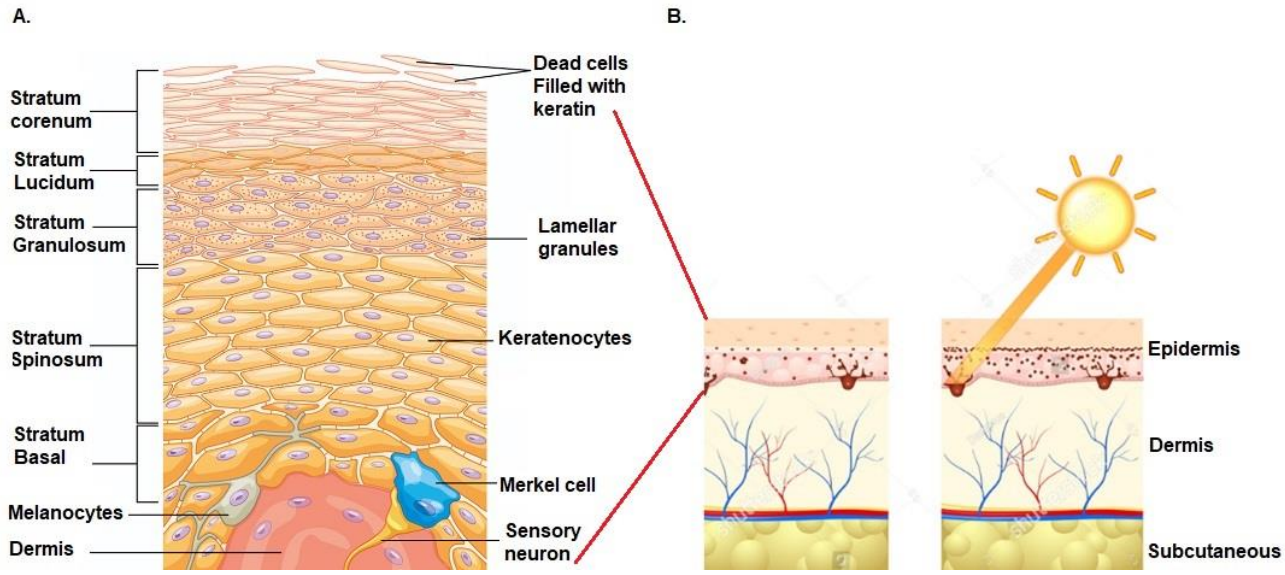

Figure 6. A. Layers of the Epidermis. The epidermis of thick skin has five layers: stratum basale, stratum spinosum, stratum granulosum, startum lucidium, and stratum corneum B. The response of melanocytes to UVR. Adapted from: lumenlearning.com

Chromatin structure Protects DNA

It has been shown in the ’70s and ’80s that chromatized DNA *in vitro* is more protective than the necked DNA in terms of UV-induced photolesions (Smerdon et al., 1978). First, due to its structural conformation, the chromatin organization works as a protection against DNA damages by minimizing the probability of direct hits in DNA. Second, the chromatin excludes water from DNA thereby reducing water radiolysis in direct vicinity of the biomolecule. For example, the hydroxyl radical, frequently produced through the water radiolysis, has an average diffusion distance of 6 nm in the nuclear environment (Roots and Okada, 1975). Thus, reducing the concentration of hydroxyl radicals adjacent to the DNA will decrease DNA Damage. Furthermore, histones and other DNA-bound proteins have a role as radical scavengers and decrease the number of DNA lesions induced through the indirect effect of ionizing radiation by their capacity to donate hydrogen atoms. Besides their role in limiting the formation of DNA lesions, histones and other non-histone DNA-bound proteins within chromatin are intimately involved in the regulation of the signaling network and DNA damage response, governed by posttranslational modifications such as phosphorylation, acetylation, and methylation, thoroughly reviewed by Hunt and colleagues (Hunt et al., 2013).

Research Goals

Chromatin plays an important role in mediating the response to different stress stimuli at different levels of the nucleosome components, histone variants, and other proteins and factors in euchromatin and heterochromatin. Based on the Access-Repair-Restore (ARR) model (Polo and Almouzni, 2015; Smerdon, 1991), the first response after the stress is to recognize and access the site of damage, in other words chromatin relaxation. Chromatin relaxation and accessing of the damage site is carried out by protein stripping of chromatin to expose DNA lesions. This is carried out by nucleosomal sliding away from the damage site by the function of ATP-dependent chromatin remodelers, histone-modifying complexes, non-core histone proteins, such as the linker histone H1, High-mobility group (HMG) proteins, isoforms of the hetero-chromatin protein 1 (HP1), and covalent modifications or post-translational modifications (PTMs) of the core histones.

The access and repair steps are somewhat overlapping. Accessing the damage site is combined with repair factors. All lesions have their own repair factors and repair mechanisms. In UV-induced stress, which creates CPDs, 6-4PPs, and 8-oxo-DG lesions can be repaired by nucleotide excision repair (NER) and base excision repair (BER) respectively, while ionizing-induced stress which creates double strand breaks (DSB) and single strand break (SSB), can be repaired through homologous recombination repair (HRR) and nonhomologous end joining (NHEJ) pathways (Soria et al., 2012). Upon repair, chromatin is restored to the pre-stress steady state, a step that is also carried out by chromatin modifiers, remodelers, and chaperons.

Finally, cells that fail to repair the DNA damage with extensive lesions are removed by apoptosis. DNA lesions that result from certain types of stresses that cannot undergo apoptosis lead to genetic instability and cause cell transformation. Based on the ARR model, chromatin needs to unfold to repair the damaged site, and it is believed that chromatin compaction restricts the ability of DNA damage response proteins to access the site of damage (Dinant et al., 2008).

Nonetheless, a recent study showed global chromatin compaction in the colon cancer cell line (HCT116) after γ-irradiation and suggested that it happens following DSB formation. Therefore, although there is localized chromatin unfolding to facilitate repair, the bulk genome becomes rapidly compacted, which was suggested to be caused by linker histone phosphorylation and hypothesized to protect cells from further damages (Hamilton et al., 2011). Another recent *in vivo* and *in situ* study also demonstrated that condensed chromatin has fewer DSBs induced by γ-rays and heavy ions and is less susceptible to attack by chemical agents such as cisplatin, and it was suggested that genomic DNA compaction plays a vital role in maintaining genomic integrity (Takata et al., 2013).

The above mentioned studies indicated that there is chromatin compaction after γ-irradiation *in vito* and *in vivo,* but Takata group did not show a clear mechanism for this compaction, nor did they find a direct link between the chromatin compaction and DNA protection. Therefore, our main research goal was to demonstrate the effect of an environmental genotoxic agent, specifically UV-radiation, on chromatin compaction. We wanted to explore if there is chromatin compaction after UV irradiation and if this compaction will result in a reduction of newly formed photolesions we also tested

whether this DNA protection mechanism, unlike other known protection mechanisms that were reported may happen in seconds or minutes and not on long timeline scale such as hours to days (Miyamura et al., 2007; Wasmeier et al., 2008). We also explored the mechanism that leads to potential UV-induced DNA compaction.

CHAPTER II

A Paper to be submitted for Publication in

The Journal Cell

Calcium-Dependent Global Chromatin Compaction Protects DNA From UV Inflicted Damage

Mohammad Abbas, Rituparna Sinha Roy, Mohammed Farhan Lakdawala, Mangalam Subramanian, LaTandra Lawrence, Chris Buliga, Tina Gumienny, and Michael Bergel

From the Department of Biology, Texas Woman's University, Denton, Texas 76204

Calcium-Dependent Global Chromatin Compaction Protects DNA From UV Inflicted Damage

Mohammad Abbas, Rituparna Sinha Roy, Mohammed Farhan Lakdawala, Mangalam Subramanian, LaTandra Lawrence, Chris Buliga, Tina Gumienny, and Michael Bergel*

* Correspondence: Michael Bergel, Department of Biology, Texas Woman's University, 304 Administration Drive, Denton, Texas, 76204, USA, Tel: 940-898-2471; Fax: 940-898- 2382; E-mail: MBergel@twu.edu

SUMMARY

Eukaryotic genomes are packaged into chromatin, which is the physiological substrate for all DNA-mediated functions, including DNA damage repair. At the DNA damage site, chromatin organization undergoes critical rearrangements during the DNA damage repair process. These rearrangements surrounding lesion site must include three steps: providing access to the repair factors, repair, and restoring the pre-lesions chromatin architecture. However, little is understood about the mechanism that orchestrates chromatin changes following UV irradiation. Here, we demonstrate that an environmental genotoxic agent, UV radiation, causes immediate and global chromatin compaction in HeLa cells and that this compaction results in a robust reduction in the newly formed lesions. Our data suggest that calcium cation influx after UV irradiation may direct the chromatin compaction. We demonstrate that chromatin compaction upon UV irradiation is conserved and widespread from the human HeLa cell line, through primary human cells to *C. elegans.*

INTRODUCTION

Chromatin is dynamically modified to regulate appropriate cellular pathways involved in DNA metabolism: replication, transcription, repair, and recombination. The dynamic state of chromatin can be influenced by cellular and environmental agents, which trigger the conformational changes that make the chromatin more open, and this unwrapping transiently expose buried DNA sites for access to repair proteins and factors (Smith and Workman, 2012). The conversion between unfolded and compacted chromatin states is dynamic and rapid. Any process that requires access to DNA must conquer these chromatin natural structural barriers (Kornberg and Lorch, 1999b). Among these environmental stresses is UV radiation, which leads to the formation of several types of dimeric lesions, including cyclobutane pyrimidine dimers (CPD) and (6-4) photoproducts (Friedberg et al., 2006; Goodsell, 2001). Both lesions distort DNA's structure, introducing kinks, and thereby impeding DNA transcription and replication (Friedberg, 2003). If these lesions are not repaired before replication, they may

result in mutations. In addition, UV induces formation of different reactive oxygen species (ROS), which cause oxidative damage that can indirectly form lesions or can form 8-oxo-deoxyguanine (8-oxo-dG) lesions (Cadet et al., 2009; Dahle and Kvam, 2003; Pillai et al., 2005).

Several known molecular and physiological responses that can be initiated upon UV radiation. One of the known physiological responses upon radiation is the activation of signaling pathway (Bellono et al., 2013)that leads to hyperpigmentation in the human melanocytes (Miyamura et al., 2007; Moan et al., 2012). Human skin detects the UV component of the sunlight through the photoreceptor rhodopsin, which is also expressed in melanocytes (Wicks et al., 2011). The signaling pathway induces calcium influx in melanocytes via the ion channel transient receptor potential A1 (TRPA1) and activates phosphodiesterase C, which leads to early melanin synthesis and redistribution in epidermis to protect cell layers beneath the melanocytes (Bellono et al., 2013). This long-term mechanism protects the cellular genome from UV light-induced DNA damage. Recent studies have demonstrated that γ-irradiation induced DNA damage in HCT116 cells triggers the phosphorylation of the chromatin associated proteins KAP1 and H2AX (Hamilton et al., 2011). This response was accompanied by genome-wide compaction of bulk chromatin fibers that was suggested to protect cells from further damage while they are repairing other damaged regions (Hamilton et al., 2011). Furthermore, when compacted chromatin *in situ*, can protect from gamma radiation and genotoxic chemicals such as neocarzinostatin (NCS) (Hamilton et al., 2011). Although it has been suggested that chromatin compaction protects DNA *in vivo*, not only *in vitro*, however to the best of our knowledge it has never been demonstrated. Furthermore, it has not been shown that the same environmental genotoxic agent that causes a chromatin compaction in the cells, and compaction subsequently protects the DNA from further damage. Furthermore, previous studies addressed the local chromatin status and remodeling after UV radiation (Rastogi et al., 2010). Insufficient research has been done to study the global response of chromatin after UV radiation.

Cations may promote chromosome condensation by counteracting the negative charge of DNA *in vitro* and *in vivo* (Gan and Schlick, 2010; Korolev et al., 2010; Korolev et al., 2012). Monovalent cations, divalent cations, and polyamines that promote nucleosome folding have been also identified by *in vitro* nucleosome arrays (Grigoryev et al., 2009; Korolev et al., 2012). Specifically, calcium ions have been shown to be involved in chromatin compaction *in vitro* and associated with mitotic chromosome condensation (Kahl and Means, 2003; Skelding et al., 2011; Strick et al., 2001). However, all previously mentioned studies were not linked to global cellular stress-induced chromatin compaction.

Here, for the first time, we demonstrate that an environmental genotoxic agent, UV radiation, causes an immediate and global chromatin compaction in cells and that this immediate compaction results in a robust reduction in the newly formed lesions, This DNA protection is occurring in a matter of second or minutes unlike other known protection mechanisms that respond slower and provide a long-term

defense (hours to days) (Miyamura et al., 2007; Wasmeier et al., 2008). To confirm that the chromatin compaction has a causal role on DNA protection, we demonstrated that protection is achieved also by the compacted mitotic chromosomes.

By chelating cellular calcium, we further demonstrated that influx of calcium cations following UV irradiation mediates the global chromatin compaction and DNA protection. We further demonstrated that this response is widespread and conserved from human HeLa cells, through primary human melanocytes, to *C. elegans*.

The existing dogma is that following UV irradiation or gamma radiation, chromatin has to unfold to allow access for DNA repair machinery (Dinant et al., 2012; Gospodinov and Herceg, 2013; Green and Almouzni, 2002; Polo and Almouzni, 2015; Soria et al., 2012). Our results, however, show that on a global scale, the chromatin is being condensed.

Results

UVC Induces a Global Chromatin Condensation in HeLa S3 Cells and NIH2/4 Cells

Recent studies have shown that chromatin undergoes a dramatic global compaction in response to DNA damage caused by γ-radiation (Hamilton et al., 2011; Takata et al., 2013). To investigate whether UV radiation is also induces chromatin compaction, HeLa S3 cells were irradiated with 30 J/m^2 (164 seconds) and HeLa cells nuclei were collected at different time points after UV irradiation and partially digested with micrococcal nuclease. DNA was then purified from digested chromatin from the non-irradiated control samples, and from the UV-C treated samples. The DNA fragments sizes representing the nucleosomal ladder were then analyzed by agarose gel electrophoresis and ethidium bromide staining (Figure 1A). The results showed that the chromatin was globally and rapidly compacted as could be demonstrated, five minutes after irradiation. Four to twenty-four hours after irradiation, the chromatin returned to the pre-UV irradiation compaction steady state. UV irradiation in different mammalian cell lines activates a complex signaling network that leads to apoptosis (Chathoth et al., 2009; Kulms and Schwarz, 2000). During the apoptosis process, the chromatin compaction shifts from a heterogeneous form to an inert highly condensed form that is subsequently fragmented and packaged into condensed bodies called apoptotic bodies (Lin et al., 2016). To determine if UV-C radiation stimulates an apoptosis-dependent chromatin condensation immediately after UV irradiation, the level of active caspase 3, an early apoptotic marker, immediately after UV irradiation was assessed. HeLa S3 cells were UV irradiated at 30 J/m^2 and cell lysates from various time points after UV irradiation were subjected to Western blotting analysis using an antibody against active caspase 3. This assay allowed us to compare the time and kinetics of apoptosis versus the kinetics of chromatin compaction. Results showed that there was no active caspase detectable five and ten minutes after UV irradiation. The earliest active caspase 3 bands could be detected 4 hours to ten hours after UV irradiation. Thus, the immediate chromatin compaction five to ten minutes after UV-irradiation is inconsistent with the et of apoptosis (Figure 1B). As additional experimental approach to test chromatin compaction after UV irradiation, we used

NIH2/4 cells that are stably transfected with an array of 256 repeats of Lac operon sequence (LacO) that can bind multiple copies of Lac repressor (LacR) fused to CFP (LacR-CFP). Fusion proteins containing the LacR-CFP expressed from a transiently transfected plasmid bind to the LacO sites and can allowing visualization of chromatin structural changes array in living cells (Soutoglou and Misteli, 2008; Tumbar et al., 1999) (Figure 1C, schematic drawing demonstrates LacO: LacR-CFP interaction). In the non-treated cells containing of LacO, the LacR-CFP formed a small, compact spots in the nucleus of the cells (Figure 1D, right panel). UV irradiation of the NIH2/4 cells with UVC (30 J/m^2) (Figure1D, middle panel) or UVB (300 J/m^2) (Figure1D, left panel) led to a significant chromatin compaction. Array compaction was determined by measuring the longest diameter of the LacO: LacR-CFP specks before and after UVC or UVB irradiation (Figure 1E). Nuclear lamins associated with chromatin/histone and play a crucial role in chromatin organization during the cell cycle (Dechat et al., 2009; Dillon, 2008; Fraser and Bickmore, 2007; Kalverda et al., 2008; Mateos-Langerak et al., 2007; Misteli, 2007; Trinkle-Mulcahy and Lamond, 2008). We predicted the nuclei diameter and volume will decrease as the condensing chromatin pulls in the nuclear membrane after UV irradiation. Thus, we examined whether the chromatin compaction upon UV irradiation influences the HeLa cell nuclei diameter and volume. HeLa cells were irradiated with 30 J/m^2 and stained with Hoechst dye and the diameter of the nuclei were measured before and five minutes after UV irradiation. We were able to detect a significant reduction in the volume of irradiated nuclei further supporting that UV radiation induces chromatin compaction (Figure 1F). In summary, our data clearly demonstrate a global chromatin compaction and nuclear diameter reduction immediately after UV irradiation. The compaction of chromatin post UV irradiation was constant between human cells (HeLa cells) and mouse cells (NIH2/4) and was induced by both UVC and UVB.

Chromatin compaction protects against further DNA damage by UV irradiation

In previous studies, chromatin compaction was shown to play a key role in protection against double-strand breaks (DSBs) generated by γ-rays and other types of DNA damages in vitro and in situ (Cann and Dellaire, 2011; Hamilton et al., 2011; Takata et al., 2013; Tan and Lan, 2016) To determine whether UV irradiation could protect chromatin from further damage, we established a double irradiation protocol in which HeLa S3 cells were irradiated with 30 J/m^2, 15 J/m^2 or twice with 15 J/m^2 with a five minute break in between irradiation. Our hypothesis was that if compaction of chromatin protects DNA from further damage then the treatment of irradiation of 15 J/m^2 twice with 5 minutes break would allow chromatin compaction prior to the second treatment resulting in a significantly less damage than the 30 J/m^2 irradiation. DNA was purified immediately after irradiation (time 0), and 7 and 20 hours after UV irradiation. The amount and the kinetics of cyclobutane pyrimidine dimer (CPDs) and their removal rate from DNA were analyzed by southwestern blotting for the analysis of 6-4photoproducts (6-4PPs). DNA was purified immediately after irradiation (time 0), and 2, 4 and 10 hours

after UV irradiation. DNA was slot blotted onto a nylon membrane and probed with monoclonal antibodies against CPDs or 6-4PP (Figure 2A and 2C). The negative control was DNA from non-irradiated cells. The CPD and 6-4PP levels were standardized against the total DNA levels by staining the membranes with ethidium bromide. CPD/DNA and 6 -4PP/DNA ratios, were determined using spot densitometry of CPD and 6- 4PP blots and ethidium bromide membranes. Results showed that cells that were double irradiated at 15 J/m^2 with five minutes break had a significant lower CPDs and 6-4PPs rate in comparison to cells subjected to 30 J/m^2. Moreover, the results indicated that the cells irradiated with 15 J/m^2 and twice with 15 J/m^2 with a five-minute break between had almost the same initial level of lesions immediately after UV irradiation and they had the similar capacity to remove UV-induced DNA lesions over time (Figure 2B and 2D). The amount of CPD lesions increased after 7 hours, and we speculate that this increase is due to the reactive oxygen species (ROS) that can be generated by UV which play role in CPD formation (Herrling et al., 2006; Hochberg et al., 2006).

Chromatin compaction and protection commence immediately upon UV irradiation and mitotic chromosomes are more protected from the damage caused by UV irradiation.

To demonstrate whether the chromatin compaction and protection from further damage initiates immediately upon irradiation or a minimal time is required for compaction and then protection will be achieved, intact HeLa cells S3 and naked DNA extracted and purified from non-irradiated HeLa S3 cells were irradiated with a range of UVC doses, but with different UVC intensities; low UVC intensity and high UVC intensity. Low UVC intensity required more time than high UV intensity to produce the same UV joulage.

Intact cells were irradiated with 15 J/m^2, 30 J/m^2 and 45 J/m^2 with two different intensities (0.094 and 0.559 J/m^2/s). DNA was purified and was slot blotted onto a nylon membrane, probed with monoclonal antibodies against CPDs (Figure 3A and 3C). The CPD levels for both intact cells and naked DNA were standardized against the DNA levels by staining the membranes with ethidium bromide (Figure 3B and 3D). Results showed that cells that were irradiated with a lower UV intensity had a lower level of CPDs in comparison to cells irradiated with a higher intensity. This result supports the hypothesis of an immediate compaction of chromatin. Thus, the longer time it takes to deliver the dose of UV the more compaction of chromatin is achieved and fewer photolesions accumulation occurs. On the contrary, the irradiated naked DNA showed no difference between lower and higher intensities of UV irradiation which suggest that the chromatin structure is indispensable for DNA protection.

We demonstrated a correlation between the UV-induced compaction of chromatin and the protection of the DNA from further damage in vivo. However, the question was whether the compaction of chromatin is the cause for the protection or there is another factor induced by UVR that elicits the DNA protection. Therefore, we decided to test another cellular condition that involves chromatin compaction that is not induced by UVC: Are the mitotic chromosomes more protected than the interphase decondensed chromatin? To address this question, we arrested HeLa S3 cells in mitosis by incubation with

nocodazole (Downing, 2000; Jordan and Wilson, 1998). Cells lysates were collected from mitotically arrested cells (synchronized) and non-arrested cells (non-synchronized) and the level of mitotic cells were confirmed by western blotting with a mitosis-specific marker anti-phosphohistone H3 antibodies (Bedekovics et al., 2018) (Figure 3E) and Mitotic Index was also calculated based on the number of metaphase cells that had been scored (Figure 3F). The synchronized cells were irradiated with 15 J/m^2 and 30 J/m^2 and DNA was purified immediately after irradiation (time 0), and 7 and 20 hours after UV irradiation, those time points are standard time interval to compare the photolesions removal by NER, and the amount and the kinetics of cyclobutane pyrimidine dimers (CPDs) removal from the DNA were measured by southwestern blotting. DNA was slot blot onto a nylon membrane, probed with monoclonal antibodies against CPDs (Figure 3G and 3H). We found that the more compact chromatin (mitotic chromosomes) are more protected from photolesions than the decondensed interphase chromatin suggesting that chromatin compaction protects genomic DNA against UV-induced damage whether it is compacted due to mitosis or due exposure to UV radiation.

Potential mechanisms that facilitate chromatin compaction in HeLa cells following UV irradiation

Acetylation levels after UV irradiation

Histone acetylation and histone deacetylation on lysine residues in the N-terminal tails of the core histones are considered epigenetic marks of chromatin that are associated with unfolded or compacted chromatin, respectively (Barnes et al., 2005; Kornberg and Lorch, 1999a; Ruan et al., 2015). We, therefore, we wanted to test the hypothesis that the UV-induced chromatin compaction is associated and may even be caused by core histone deacetylation.

To assess the level of core acetylation following UV irradiation, HeLa S3 cells were UV irradiated at 30 J/m^2 and whole cell lysates were prepared at different time points after the irradiation. The lysates were then subjected to analysis of acetylation levels of H3K9, H3K14, and H4K5 by western blotting with the appropriate antibodies. The western blot analysis and the graphical presentation (Figure 4A) revealed a global wave of deacetylation reaching its maximum 4 hours after UV irradiation in the three sites tested. After the four hours point, there was a gradual increase in the acetylation of the three residues back to the pre-UV steady-state level. This phenomenon of returning to the pre-UV acetylation steady-state levels was also observed in DT40 wild-type chicken cells (data not shown). In summary, these results demonstrated a post-UV core histone deacetylation wave followed the chromatin condensation; however, the wave of core histone deacetylation progressed much slower than the condensation of chromatin and hence is not likely to cause it.

To determine if this wave of deacetylation play a causal role in chromatin compaction, HeLa S3 cells were treated with Trichostatin A (TSA) for 20 hours, TSA inhibits class I and II histone deacetylases (HDACs) (Imai et al., 2000; Vanhaecke et al., 2004), then HeLa S3 cells were irradiated with 30 J/m^2 and HeLa cells. Nuclei and cell lysates were

collected at 5 and 10 minutes after UV irradiation and non-UV control samples were then subjected to western blotting analysis using the anti-H3K9ac or anti-H4K5ac (Figure 4B). Western blotting results showed hyperacetylation of H3K9 and H4K5 in the TSA treated cells as expected. The nuclei from the control non-irradiated cells and from the UV-C treated cells were partially digested with micrococcal nuclease and then the DNA chromatin was purified. The purified DNA was analyzed by agarose gel electrophoresis and stained by ethidium bromide staining (Figure 4C). Cells not treated with TSA served as a negative control. At the peak of chromatin compaction 5-10 minutes, post-UV irradiation, TSA treatment that caused hyperacetylation of core histone did not inhibit chromatin compaction. Thus, we concluded that core histone the deacetylation is not the cause for the UV-induced chromatin compaction.

H1 Linker histone and Heterochromatin protein 1 are not involved in chromatin compaction after UV irradiation

H1 linker histone and heterochromatin protein 1 play essential roles in the compaction of both euchromatin and heterochromatin (Hergeth and Schneider, 2015; Zeng et al., 2010). The basic C-terminal domain (CTD) and N-terminal domain (NTD) of H1 bind to and neutralize the negatively charged linker DNA on either side of the nucleosome, thereby facilitating euchromatin compaction (Roque et al., 2016; Schlick et al., 2012; Schmitges et al., 2011). Heterochromatin protein 1 (HP1) and tri-methylation of histone H3 at lysine 9 (H3K9me3) are also associated with a highly compacted heterochromatin in which H3K9me3 serves as a binding site for heterochromatin protein 1 (HP1) (Lachner et al., 2001), which aids in the formation of heterochromatin through oligomerization (Nielsen et al., 2001). To determine whether chromatin compaction following UV irradiation is related to increased chromatin-bound levels of linker histone H1 (H1), heterochromatin protein 1 (HP1-α) or the tri-methylation of histone H3 on lysine 9 (H3K9me3). HeLa S3 cells were cross-linked with 1% formaldehyde before and 5 and 10 minutes after UV irradiation and nuclei were isolated and chromatin was fractionated after reversing the crosslinking by heating for 30 minutes at 65 °C and dialyzed overnight (to dilute the reverse crosslinking 5M NaCl solution). H1, HP1-α and H3K9me3 levels were analyzed by Western blotting using an antibody against H1, HP1-α H3K9me3 (Figure 4D and 4 E). H3K9me3The results showered no significant increase in H1, HP1-α and H3K9me3 levels after UV irradiation (Figure 4D). This result suggested that the total levels of chromatin associated H1 and HP1 proteins were similar between the condensed and decondensed chromatin, indicating that the chromatin compaction and protection are H1 and HP1-independent.

The UV-induced chromatin compaction is photoproducts site-independent.

We have demonstrated chromatin compaction following UV irradiation by micrococcal nuclease digestion and LacO: LacR-CFP array experiments. To further study if the chromatin compaction takes place only adjacent to photoproducts or globally, we used global and local UV irradiation and immunofluorescence

microscopy. Local UV irradiation is a method that uses a porous membrane through which the cells were irradiated allowing visualization of DNA photoproducts within specific sites in the nucleus (Suzuki et al., 2010). The UV irradiation of the cells was done globally (without using a filter) 30 J/m^2 and locally at 100 J/m^2 through an isopore polycarbonate membrane filter (3 µm in size), which generated damage in a spotted pattern. The high UV dose used (100 J/m^2) was necessary to visualize the permanence of CPD lesions 5 minutes after irradiation. Cells were fixed and then incubated with antibodies against CPD and stained with Hoechst as a counter stain (Figure 4E). Global UV and local UV irradiation results showed that chromatin compaction is not colocalized with areas of UV damage the (CPD foci).

The compaction of chromatin after UV irradiation is calcium-dependent

Monovalent cations, divalent cations, and polyamines are known to promote nucleosome array folding in vitro (Grigoryev et al., 2009; Vanhaecke et al., 2004). Calcium is one of the most abundant divalent cations present in cells and is known to boost chromosome condensation by neutralizing the negative charge of DNA (Gan and Schlick, 2010; Korolev et al., 2010). Divalent cations, particularly Mg^{2+} and Ca^{2+}, are known to increase during the mitotic phase of the cell cycle when chromosome compaction occurs (Strick et al., 2001; Tombes and Borisy, 1989) . In addition, It has been shown that solar ultraviolet radiation leads to rapid calcium mobilization in melanocytes (Bellono et al., 2013) suggesting ca^{+2} changes may trigger chromatin compaction. To examine the effect of Ca^{2+} depletion on chromatin compaction after UV irradiation, HeLa cells were incubated with the Ca^{2+}-chelating agents:1,2-bis(*o*-aminophenoxy)ethane-*N*,*N*,*N′*,*N′*-tetraacetic acid) (BAPTA-AM) and ethylene glycol-bis(β-aminoethyl ether)-*N*,*N*,*N′*,*N′*-tetraacetic acid (EGTA) for 45 minutes before UV irradiation. When inside the cell BAPTA-AM is cleaved by esterases to form the active form – BAPTA, whereupon it loses its ability to traverse cellular membranes, thereby trapping it within cells (Strayer et al., 1999). The calcium-chelators treated HeLa S3 cells were irradiated with 30 J/m^2 and nuclei were collected at different time points and digested with a micrococcal nuclease. Digested chromatin was extracted also from the control groups that were irradiated without Ca^{2+}-chelating agent treatment. DNA was purified and the nucleosomal ladder was analyzed by agarose gel electrophoresis and stained by ethidium bromide staining (Figure 5A). The micrococcal nuclease analysis demonstrated that calcium depletion leads to less compacted chromatin after UV irradiation. To further confirm the micrococcal nuclease results, we used fluorescence microscopy to examine the relationship between Ca^{2}+ levels before and after UV irradiation. HeLa cells were treated with BAPTA-AM and EGTA along with fluorescent calcium indicator called Fluo4-AM to image the changes in chromatin compaction, cells were fixed, and images were taken with no UV irradiation (Figure 5B right panel) and after UV irradiation (Figure 5B left panel). The cells treated with both chelators demonstrated a reduced Fluo4-AM signal. Thus, the chelators were effective in blocking some of cellular calcium when the cells treated with BAPTA and EGTA separately there was a

reduction in chromatin compaction. Interestingly, there was a higher decrease in the compaction of chromatin, as seen with Hoechst staining when cells were treated with both BAPTA and EGTA. To explore whether chromatin compaction after UV irradiation is associated with a change in Ca^{2+} concentration, HeLa cells were labeled with the $Ca+^{2}$ Fluo-4 AM and intracellular and nuclear calcium intensity were measured before and after 30 J/m^2 irradiations (Figure 5C). Results revealed that there is a significant increase in both cytoplasmic and nuclear calcium (Figure 5D) 5 minutes after UV irradiation. These results indicate that calcium cation influx contributes to promoting chromatin compaction after UV irradiation.

Calcium ion depletion leads to reduced chromatin compaction after local UV irradiation and a decrease in nuclear diameter after UV irradiation.

To investigate the effect of different calcium chelators on compacted chromatin foci upon local UV-irradiation the NUCLEAR-ID Green chromatin condensation detection kit was used to stain the condensed chromatin by this DNA intercalating dye. HeLa cells were grown on a glass slide and incubated with the Ca^{2+}-chelating agents BAPTA-AM or EGTA separately, or together, and then locally irradiated at 100 J/m^2 through an isopore polycarbonate membrane filter (with pores 3 µm in size). Cells that were not irradiated and not treated with Ca^{2+}-chelating agents BAPTA-AM and EGTA served as negative controls. Cells were observed under a fluorescence/confocal microscope with a filter set for GFP/FITC (Figure 6A). When the cells were irradiated, we observed higher amounts of nuclear staining compared to the unirradiated cells. However, when the cells treated with chelating agents independently there was a reduction in the amounts of nuclear staining indicating less chromatin compaction. As in the previous assay, there was considerable decrease in the compaction of chromatin when cells were treated with both BAPTA and EGTA. Since calcium ions chelation decrease chromatin compaction after UV irradiation, next we wanted to examine whether the calcium chelating agents influences the HeLa cell nuclei volume and diameter. HeLa cells were incubated with calcium chelator, irradiated with 30 J/m^2, and stained with Hoechst dye and their nuclear diameters were measured. A significant reduction in the nuclei diameter was detected after UV irradiation; however, cells that were incubated with chelators and irradiated had no any significant decrease in their nuclear diameter (Figure 6B). These results evidently demonstrate that the mechanism of a chromatin compaction and nuclear diameter reduction are calcium-dependent mechanism.

Calcium ion depletion impedes the chromatin compaction protection mechanism and impairs the nucleotide excision repair after UV irradiation

To test the how calcium depletion affects the CPD and 6- 46PP photolesions removal rate after UV irradiation. HeLa S3 incubated with a combination of Ca^{2+}-chelating agents BAPTA-AM and EGTA and then irradiated with 30 J/m^2, 15 J/m^2 and twice with 15 J/m^2 with a five-minute break between. DNA was purified immediately at different time points after UV irradiation. DNA was slot blotted onto a nylon membrane and probed with monoclonal antibodies against CPDs or 6-4PP (Figures 7A and 7C). The negative

control was DNA from non-UV irradiated cells). The CPD and 6-4PP levels were standardized against the DNA levels by staining the membranes with ethidium bromide. CPD/DNA and 6 -4PP/DNA ratios were determined using spot densitometry of CPD and 6- 4PP blots and ethidium bromide stained DNA membranes. Results showed that cells that were incubated with calcium chelators lost their ability to protect DNA from further damage and lost their ability to remove UV-induced DNA lesions over the course of time (Figures 7B and 7D). These results support the pivotal and perhaps the causal role of calcium cations cellular influx in chromatin compaction and DNA protection in UV-induced NER function.

Discussion

In the present study, we found that chromatin is globally compacted after UVC irradiation, and this compaction protected genomic DNA from further damage. Importantly, this study suggests the causal involvement of Ca^{2+} ions in chromatin compaction and following DNA protection. We ruled out as possible mechanism for chromatin compaction TSA-inhibited HDAC I and II classes, H1 and HP1, as well as H3K9 methylation. However, we cannot rule out additional mechanisms that nay contribute to this compaction phenomenon, such as sirtuin mediated descetyaltion. Based on our results and finding by others (Hamilton et al., 2011; Strayer et al., 1999), we propose that cellular DNA protection by chromatin compaction represent a universally conserved function, from human cell lines like HeLa cells through human melanocytes to *C. elegance*, in a large variety of stresses. Several *in vitro* studies have shown that chromatin condensation by polyamine or monovalent cations also protected genomic DNA and suppressed more damage induced by gamma radiation (Douki et al., 2000; Spotheim-Maurizot et al., 1995; Warters et al., 1999). Here, we demonstrated that calcium ions are crucial in chromatin compaction and DNA protection *in vivo*, and that calcium is required and essential for nucleotide excision repair.

Although we emphasized the importance of chromatin compaction in the maintenance of genomic DNA integrity by the robust reduction in both CPD and 6 -4 PP photolesions, chromatin compaction might interfere with DNA damage repair due to a reduction in chromatin accessibility. However, recent studies observed local nucleosome fluctuations in living mammalian cells, and this fluctuation increases chromatin accessibility, especially in compacted chromatin regions (Hihara et al., 2012)

According to our model (figure 8), upon UV irradiation calcium influx from different cellular and extracellular calcium storages neutralizes the negatively charged DNA phosphate group, which leads to chromatin compaction, and in turn, this response causes the pulling of the nuclear envelope, which results in nuclear diameter and volume reduction.

Furthermore, we reported that chromatin decondensed and returned to its pre-UV steady-state four to twenty-four hours after UV irradiation, increasing chromatin accessibility for global repair.

Despite the ability of divalent calcium cations to promote the chromatin compaction upon UV irradiation, we cannot rule out the involvement of other monovalent, divalent, or polyvalent cations, or other components.

Furthermore, it is important to emphasize that our findings provide a theoretical basis for a possible new generation of sunscreen creams. Sunscreens include physical ingredients that include the minerals titanium dioxide and zinc oxide that block and scatter the rays before they penetrate human skin and chemical ingredients like avobenzone and octisalate, which absorb UV rays before they can damage the skin. Our findings provide a theoretical basis to add agonist chemical that will induce the function of rhodopsin that senses the UV irradiation and activates G protein, which activates downstream signaling cascade to facilitate calcium release from the smooth endoplasmic reticulum or other depots to initiate and enhance chromatin compaction and protection.

Finally, our study provides strong evidence that intensive and prolonged exposure to the sun can be safer than shorter but frequent times of exposure. Our studies explain the molecular mechanism for the phenomenon of higher skin cancer rate among people who have several short exposures to the sun during the day in comparison to individuals that have one prolonged exposure.

Methods Details

Cell culture

Human HeLa S3 cells were used for micrococcal nuclease digestion, Southwestern experiments, and Western blotting. Human HeLa cells were used for immunostaining after local UV irradiation and calcium intensity measurement. NIH2/4 mouse embryonic cell line, which carries an array of 256 copies of the LacO binding sequence and 96 copies of the tetracycline response element sequence, was a gift from Dr. Tom Misteli (NIH). Cells were maintained in Dulbecco's modified Eagle's medium (Gibco/BRL) supplemented with 10% heat-inactivated fetal bovine serum (Gemini) and 1% Penicillin-streptomycin. The cells were grown in tissue culture flasks or spinner flasks in an incubator with 5% CO2 and 100% humidity at 37 °C.

Western blot

Whole cell lysates were fractionated on a 12% or 15% SDS polyacrylamide gel. The proteins were transferred to PVDF membranes (Millipore) using a Bio-Rad semidry transfer cell. Membranes were probed overnight at 4ºC with one of the following primary antibodies: anti-Histone H1 (Santa Cruz Biotechnology), anti-phospho-H3S10 (Upstate), anti-acetyl-H3K9 (Millipore), anti-acetyl-H4K5 (Santa Cruz Biotechnology), anti-trimethyl-H3K9 (Millipore), anti-Caspase 3 (Millipore), and anti-HP1α (Millipore). The bound antibodies were detected with horseradish peroxidase-conjugated secondary antibodies and proteins were visualized using an ECL Plus kit (Amersham Biosciences).

UV irradiation

Prior to irradiation, HeLa S3 cells were grown in a spinner flask and then centrifuged at 500 x g for 5 minutes followed by two washes with PBS (Thermo Fisher). The cells were then resuspended in PBS, placed in large tissue culture plates 30 ml capacity, and then incubated with a thin layer PBS during UV irradiation. Cells were exposed to global UV irradiation with Philips TUV lamp (predominantly 254 nm) for different doses and intensities. For local UV irradiation, HeLa regular cells grown on coverslips were covered with a porous isopore polycarbonate filter with pores of 3.0 µm diameter (Millipore) and irradiated with 100 J/m^2 doses. Following UV irradiation, the filter was removed, and the cells were fluorescently labeled or immunostained. A UV-C sensor (UV Products) was used to calibrate the fluency rate of the incident light.

Southwestern analysis of photoproduct levels

HeLa S3 cells were grown and maintained in a spinner flask in presence or absence of calcium chelators. The cells were washed twice, resuspended in PBS, and then irradiated at the desired joulage in a 150 mm polystyrene petri dish. Following UV irradiation, fresh media was added and the cells were incubated in spinner flasks maintained in an incubator under normal growth conditions. At different time points (0 hour – 24 hours), DNA was extracted using proteinase-K buffer and purified by phenol-chloroform method (Gross-Bellard et al., 1973). The extracted DNA (1 µg) was slot-blotted onto Hybond- N+ membranes (GE Lifesciences). The DNA was cross-linked by a 30 minutes incubation in an 80 °C vacuum-oven. The level of CPDs and 6-4PPs and their removal rates were assessed using mouse anti-CPD (Clone: TDM2) and mouse

anti-6-4PPs monoclonal antibodies as described by Schwarz et al (Schwarz et al., 2002). Anti-CPD Clone: TDM2 was a gift from T. Tadokoro, Department of Dermatology, Osaka University, Japan). The CPD and 6-4PP photolesions to DNA ratio was determined using spot densitometry with AlphaEaseFC (FluorChem HD2) software, version 6.0. The tests were performed in a linear range according to the calibration curve.

Fluorescent Labeling

HeLa cells were grown on glass coverslip to 70% confluence, washed twice with cold PBS, incubated with a layer of PBS, and globally or locally radiated. After irradiation, cells were fixed and lysed by addition of PBS containing 2% paraformaldehyde and 0.2% Triton X-100 while maintaining the cells on ice for 15 minutes. Cells were washed twice with cold PBS and blocked with 3% bovine albumin in PBS for 30 min at room temperature. To visualize UV-induced photoproducts, cells were washed twice with PBS, treated with 2 M HCl for 5 min at 37ºC to denature the DNA, and washed once with PBS. Cells were subsequently rinsed once with washing buffer (PBS containing 0.5% bovine albumin and 0.05% tween-20), incubated with the cyclobutane pyrimidine dimers (CPDs) primary antibody in washing buffer for 2 hours at room temperature. Cells were washed three times with washing buffer, then incubated with goat anti-mouse-FITC in washing buffer for 1 hour at room temperature followed by three washes in washing buffer. Chromatin was counterstained with Hoechst stain (5 µg/mL) (Invitrogen) for 5 minutes, and Prolong Antifade mounting medium (Invitrogen) was added before sealing the coverslip.

Isolation of Nuclei and Microccocal Nuclease Digestion

For the isolation of nuclei, HeLa S3 cells grown in suspension were centrifuged at 180 x g at 4 ºC for 5 minutes and washed twice with PBS, then resuspended in PBS and placed in 150 mm polystyrene petri dishes and irradiated. The irradiated cells were incubated in DMEM in a 37 °C incubator for different time points. Five and 10 minutes time points were incubated in ice cold PBS. For intact nuclei isolation, the irradiated cells were centrifuged at 500 x g at 4 ºC for 5 minutes. The cell pellet was resuspended in lysis buffer A (10 mM Tris-Cl (pH 7.4), 10 mM NaCl, 0.5% NP-40, and 1 mM PMSF). Cells were vortexed and then centrifuged at 500 x g at 4 ºC and resuspended in buffer A and of buffer B (10 mM Tris-Cl (pH 7.4), 3 mM $CaCl_2$, 2 mM $MgCl_2$, 1% NP-40, and 1 mM PMSF) in one to one ratio per 50 million cells. Cells then were transferred to an ice-cold Dounce homogenizer with pestle type B and 10 to 20 strokes were carried out. The lysate was then centrifuged for 5 minutes at 500 x g at 4ºC. Nuclei were stored in glycerol storage buffer (50 mM Tris-Cl (pH 8.4), 40% glycerol, 5 mM $MgCl_2$ and 0.1 mM EDTA) at a concentration of 50 million cells/ 200 µl. For micrococcal nuclease (MNase) sensitivity digests, the nuclei concentration was adjusted based on the relative absorbance of 260nm in nuclei buffer R (0.1% SDS and 0.1% NaOH). Nuclei (500 µg) were digested with 50 units of micrococcal nuclease (Roche) for eight minutes at 25°C in 1 ml of digestion buffer (85 mM KCl, 1 mM $CaCl_2$, 5 mM PIPES (pH 7.5), 5% sucrose). Digested chromatin was extracted from UV irradiated cells with and without calcium chelators, and then purified using phenol: chloroform. DNA concentration was measured at 260 nm, and 5 µg of isolated DNA from different samples was fractionated

by 2% TAE agarose gel electrophoresis followed by 0.5 µg/ml ethidium bromide staining. Gel analysis was carried out by using spot densitometry and AlphaEaseFC (FluorChem HD2) software, version 6.0.

HeLa cell nuclear LacO: LacR-CFP diameter measurement

NIH2/4 cells containing 256 chromosomal tandem repeats of LacO were plated on coverslips, grown to 70% confluence, washed twice with cold PBS and transfected with LacR-CFP plasmid using Lipofectamine 3000 reagent (Thermofisher Scientific). The cells were then irradiated with 30 J/m^2 and fixed with 4% paraformaldehyde for 15 min at room temperature. HeLa S3 cells were grown to about 70% confluency. The media was removed, and the cells were washed once with serum free DMEM. BAPTA-AM in DMSO (50 µM final concentration) was added to 1 ml of serum free DMEM. EGTA (50 µM final concentration) was added to 1 ml of serum free DMEM and a mixture of BAPTA-AM in DMSO and EGTA (50 µM final concentration). Cells then were incubated for 40 minutes at 37°C. The cells were washed twice with PBS and were irradiated with 30 J/m^2 with a thin layer of PBS and stained with Hoechst. Cells were then washed once with CO_2 independent medium lacking phenol red (Invitrogen) and imaged with the same media. The diameter of LacO: LacR-CFP specks as well as the HeLa S3 nuclear diameter were measured was measured using NIS-Element AR.

Core Histone Hyperacetylation and Mitotic Arrest prior to UV irradiation of cells

To hyperacetylate core histones, HeLa S3 cells grown in suspension were treated with 2 µM of trichostatin A (Sigma) for 20 hours. Cells were collected by centrifugation at 180 x g at 4ºC for 5 minutes. Cells were washed twice with PBS and then resuspended in PBS and placed in 150 mm polystyrene petri dishes. The cells were irradiated then incubated in PBS for 5 or 10 minutes and nuclei were isolated and subjected to micrococcal nuclease digestion. Additionally, whole cell lysates of each time point were collected by lysis with 1X Laemmli buffer and mini complete protease inhibitor tablet (Roche Life Sciences). For mitotic arrest, HeLa S3 cells were treated with 100 nM nocodazole (Sigma) for 20 hours. To assess mitotic arrest, cells were either lysed with 1X Laemmli buffer followed by western analysis for phosphorylated H3S10 or stained with Hoechst and the Mitotic index was measured microscopically. Mitotically arrested cells were suspended in PBS and irradiated at the desired joulage. Following UV irradiation, fresh media was added, and the cells were incubated in spinner flasks under normal growth conditions for the 0, 7, and 20-hours' time points. DNA was extracted at the desired time points (0-24 hours) and the levels of CPDs and 6-4PPs and removal rate were assessed.

Level of Chromatin-bound H1, HP1-α and H3K9me3 assessment upon UV irradiation

HeLa cells were irradiated with 30 J/m^2 then incubated in fresh medium under normal growth conditions. DNA was crossed-linked by adding 1% formaldehyde in PBS after the desired time then incubated for 10 minutes at 37ºC. Nuclei from each time point were isolated as previously described. Nuclei were resuspended in swelling buffer (25 mM EDTA and 1 mM PMSF) and incubated for 60 minutes at room temperature. Nuclei were pelleted at 500 x g at 4ºC for 5 minutes and then resuspended in 1 ml of lysis buffer (10% SDS, and 0.1M $NaHCO_3$). NaCl (5M) was added and cross-linking then reversed by heating at 65ºC for 4 hours. The lysate was dialyzed overnight in a Slide-a-Lyzer cassette (10,000 molecular weight cutoff, Pierce) against PBS in cold room. The nuclear lysate was collected and 1X Laemmli buffer were added with mini complete protease inhibitor tablet (Millipore) and heated at 94ºC for 20 minutes. Lysate was centrifuged at 10,000 X g for 2 minutes at 4ºC. Western blotting analysis was performed for anti-histone H1, anti-trimethyl-H3K9 and anti-HP1α. Non-UV irradiated sample served as a negative control.

Chromatin compaction

HeLa S3 cells were plated on coverslips, grown to 70% confluence, washed twice with cold PBS. Cells were stained with 5 µM of Nuclear ID-green staining reagent (Enzo) in 1 ml of serum free DMEM. Cells were incubated at 37°C for 20 minutes. Cells then were washed twice with PBS and covered with a very thin layer of PBS and then a porous isopore polycarbonate filter with pores of 3.0 µm diameter (Millipore) were placed during

irradiation with UVC (254 nm) 100 J/m^2 doses. Filters were carefully removed, and the cells were then washed once with PBS and stained with 0.5 µg/ ml Hoechst stain for 5 minutes, and then cells were washed with PBS and imaged in CO_2 independent medium lacking phenol red.

Calcium Ion Measurements

Calcium measurements were performed using the cell-permeable calcium specific dye, Fluo4-AM (Invitrogen). HeLa cells were grown to approximately 70% confluency, the media was removed, and the cells were washed once with serum free DMEM (Invitrogen). Cells were incubated for 40 minutes at 37°C with a mixture of Fluo4-AM (1µM final concentration) and Pluronic F-127 (0.04% final concentration) in serum free DMEM. For experiments using BAPTA-AM or EGTA, 50 µM BAPTA-AM in DMSO and 50 µM EGTA were added to the Fluo4-AM/Pluronic F-127 mixture prior to the addition of serum free DMEM. The cells were then washed once with PBS and imaged in CO_2 independent medium lacking phenol red (Invitrogen). Fluo4-AM was imaged with excitation at 488 nm and emission at 525 nm in a 37 °C chamber attached to the confocal microscope. All images were obtained using a 60x oil immersion objective, and the quantification of change in Fluo4-AM fluorescence was carried out using ImageJ software, with a region of interest drawn within the nuclear and cytoplasmic regions of cells and mean fluorescent intensity measured and compared with non UV-irradiated cells.

Figure legends

Figure 2.1: **UVC Induces global chromatin condensation in HeLa cells.** (A) Agarose gel of DNA fragments partially digested by micrococcal nuclease of control group (lane 1), 5min, 10 min, 4 hours, and 24 hours (lanes 2, 3, 4, and 5) after UV irradiation respectively. (B) cleavage of procaspase-3 into active caspase -3 in HeLa cells after different time points. HeLa cell lysates were analyzed for cleavage of procaspase-3 using immunoblot with anticasepase-3 antibodies. (C) Schematic drawing demonstrates the interaction of LacR-CFP to condensed array of 256 repeats of Lac operon (LacO) chromatin array**.** NIH2/4 cells were transfected with LacR-CFP expression plasmid for two days. The transfected cells kept unirradiated as a negative control (D) and then UVC irradiated with 30 J/m^2 and UVB with 300 J/m^2, and then fixed by 4% paraformaldehyde and visualized by confocal microscope. (E) The Bar graph indicates mean diameter of condensed array before and after UV-C and UV-B irradiation ±SE. Thirty-two cells of each treatment were examined (Mann-Whitney U test, $p < 0.05$, $n = 3$). (F) Bar graph represents HeLa S3 nuclei mean diameter after 5 minutes of UVC radiation with 30 J/m^2. (Mann-Whitney U test, $p < 0.05$, $n = 300$)

Figure 2.2: UV induced chromatin compaction is a physiological response that protect the DNA from Further damage (A) and (C) represent Southwestern analysis of CPD and 6-4PP removal in the HeLa S3 cells. Cells were UVC irradiated with a dose of 30 J/m^2, 15J/m^2 , and twice 15 J/m^2 with 5 minutes break. DNA was extracted from non-radiated cells and from cells immediately after irradiation, and 7 and 20 hours after irradiation for CPD, and DNA was extracted from non-radiated cells and from cells immediately after irradiation, and 2, 4 and 10 hours after irradiation. One µg of DNA was loaded per slot, on a slot blotter system and transferred to Hybond-N+ membrane. (A) The membranes were fixed at 80℃ for 15 minutes and incubated with anti-CPD monoclonal antibody, and with 6-4PP monoclonal antibody. The CPDs and 6-4PP levels were standardized against the DNA levels by staining the membranes with ethidium bromide. (B) and (D) represent the percent of CPD/DNA and 6-4PP/DNA that was determined using densitometry of four independents blots. The graphs represent the means (±SE) from four independent experiments. No significant differences were detected between single 15 J/m^2 and double 15 J/m^2 with 5 minutes break groups significant difference were found between 15 J/m^2 and 30 J/m^2 and between the double 15 J/m^2 and 30 J/m^2-depicted by * (Kruskal-Wallis test, $p > 0.05$). (E) Western blots displaying the caspase-3 activation after UV irradiation. HeLa S3 irradiated with a dose of 30 J/m^2, 15 J/m^2, and twice 15 J/m^2 with 5 minutes break at different time intervals. The cleavage of procaspase cannot be detected after the double 15 J/m^2 with 5 minutes break group.

Figure 2.3: Chromatin compaction upon UV irradiation immediately protects DNA from further damage and condensed mitotic chromatin is more protected than the interohase relaxed chromatin after UVR (A) Southwestern analysis of CPD levels in the HeLa S3 cells upon UV irradiation with the same joulage but different UV intensities. Cells were UVC irradiated with a dose of 15 J/m^2, 30 J/m^2 and 45 J/m^2 using 0.559 and 0.094 J/m^2/sec UV intensities. DNA was extracted from non-radiated cells and from cells immediately after irradiation for CPD, and DNA was extracted from non-radiated cells and from cells immediately after irradiation. One µg of DNA was loaded per slot and transferred to Hybond-N+ membrane. The membranes were fixed at 80℃ for 15 minutes and incubated with anti-CPD monoclonal antibody. The CPDs levels were standardized against the DNA levels by staining the membranes with ethidium bromide. (B) The percent of CPD/DNA was determined using densitometry of three independents CPD blots. Statistically significant differences were detected between the low and high intensity UV irradiated cells. (C) Southwestern analysis of CPD levels within naked DNA that was extracted and purified from HeLa S3 cells. Naked DNA were UVC irradiated with a dose of 5 J/m^2, 10 J/m^2, 15 J/m^2 , 30J/m^2 , and 45 J/m^2 using 0.559 and 0.094 J/m^2/sec UV intensities · One µg of DNA was loaded per slot and transferred to Hybond-N+ membrane. The membranes were fixed at 80℃ for 15 minutes and incubated with anti-CPD monoclonal antibody. The CPDs levels were standardized against the DNA levels by staining the membranes with ethidium bromide. (D)The percent of CPD/DNA was determined using densitometry of three independents CPD blots. No Statistically significant differences were detected between the low and high intensity UV irradiated naked DNA. (E) Western blot analysis of extracts from HeLa cells, either untreated or treated with nocodazole (100 ng/ml for 20 hours). (F) Bar chart of mitotic index of HeLa S3 cells after 20 hours Nocodazole incubation. Each value represents the mean and standard error from three different observations. (G) Southwestern analysis of CPD levels in unsynchronized and synchronized HeLa S3 (*n* = 3) at 0, 7, and 20 h post UVC (30 J/m^2) and (15 J/m^2). The CPDs level was standardized against the DNA levels by staining the membranes with ethidium bromide. (H) Quantitative percentage of CPD/DNA was determined using densitometry of three independents CPDs blots. The graphs represent the means (±SE) (*n* = 3). Single asterisk is statistically significant differences level between single 30 J/m^2 with nocodazole and 30 J/m^2, or the double asterisks indicated value that are significantly different between double 15 J/m^2 nocodazole treated and nontreated cells as determined by Kruskal-Wallis test, $p > 0.05$.

Figure 2.4: Core histones hyperacetylation, H1 linker histone (H1), heterochromatin protein 1-α are not involved with UVC induced global chromatin compaction. (A). UV irradiation induces a rapid global wave of deacetylation of core histones H3 and H4 in HeLa cells. The graph represents acetylation percent over time (hours) post UV-irradiation. The cells were irradiated at 30 J/m^2 at different time intervals. The deacetylation reached its maximum at 4 hours in respective residues: H3K9, H3K14, and H4K5. Each data point represents the mean of three independent repetitions (±SE). (B) Trichostatin A treatment forms a stable hyperacetylated H3K9 and H4K5. Cells treated with TSA for 16 hours then the cell lysates were subjected to western blotting with monoclonal antibody to the indicated histones (B). Increasing the acetylation level of core histones does not affect chromatin compaction rate after UV irradiation. (C) Agarose gel of DNA fragments partially digested by micrococcal nuclease of control group (lane 2), 5 min, and 10 min, lanes 3 and 4 respectively after 30 J/m^2 UVC irradiation. Lanes 4, 5 and 6 represent DNA fragments after TSA and UV irradiation treatment at 5 and 10 minutes. (D) Western blots of H1 linker histone (H1), heterochromatin protein 1-α (HP1- α), and tri-methyl-histone H3 Lys9 (H3K9Me3) levels after 30 J/m^2 UV irradiation. Linker histone H, HP1-α and H3K9Me3 were detected in nuclear extracts after reversing the cross linking of non-irradiated, 5 minutes and 10 minutes after irradiation. SDS-PAGE stained with Coomassie to show equal loading. (E) Bar graph indicate the level H1 linker histone (H1), heterochromatin protein 1-α (HP1-α), and tri-methyl-histone H3 Lys9 (H3K9Me3) levels after 30 J/m^2 UV irradiation. (F). Asynchronously growing HeLa S3 cells were irradiated with a dose of 30 J/m^2 , 15J/m^2 , and twice 15 J/m^2 with 5 minutes break and also were irradiated (100 J/m^2) through micropore filters. Cells were fixed five minutes post UV irradiation and immunostained with antibody recognizes CPD photolesions.

Figure 2.5: UVC irradiation leads to an increase in intracellular and intranuclear calcium, which consecutively leads to chromatin compaction. (A) Nuclease sensitivity analysis of chromatin structure after incubating HeLa cells in BAPTA, AM and EGTA calcium chelators and then UVC irradiation. Agarose gel of DNA fragments partially digested by MNase of control group (lane 1), 5min, 10 min, 4 hours, and 24 hours lanes 3, 5, 7 and 9 respectively after 30 J/m2 UV irradiation. Lanes 2, 4, 6, 8, and 10 represent DNA fragments collected after BAPTA, AM and EGTA calcium Chelators and UV irradiation treatment. (B) Calcium depletion prohibits chromatin compaction after UV irradiation. Fluo4-AM loaded HeLa cells S3 were imaged before and after UVC irradiation (30 J/m2). The increase in green fluorescence indicates an increase in free intracellular and intranuclear calcium levels. The increase in chromatin compaction (blue spots) can be seen from Hoechst staining. Increase in free intracellular and internuclear calcium upon UVC irradiation can be prevented by preloading the cells with EGTA or BAPTA-AM or both which are an intracellular and intranuclear Ca^2+ chelators. Chromatin compaction is highly reduced in presence of EGTA and BAPTA-AM (left panel). Fluo4-AM loaded HeLa cells were imaged without UVC irradiation, which serve as control for experiment panel A. (C) Fluo4-AM loaded HeLa cells were imaged before

and after UVC irradiation (30 J/m^2) and Fluo4-AM fluorescence intensity were measured in cytoplasm and nuclei. (D) Bar graphs representation of the fluo4-AM mean intensity for both cytoplasm and nuclei of HeLa S3 before and five minutes post UV irradiation. All determinations in all panels were made in the absence of extracellular calcium. Data are expressed mean ± SE; *$p \leq 0.05$, $n = 300$.

Figure 2.6: Local UV irradiation cause chromatin compaction and diminishes in presence of calcium chelators. (A). Asynchronously growing HeLa S3 cells stained with NUCLEAR-ID Green dye and then were irradiated with a dose 100 J/m^2 through micropore filters. Cells were fixed five minutes post irradiation. Hoechst dye was used as a counter stain. Spotty pattern was observed upon local UV radiation and calcium chelators reduce the local compaction. UV irradiation reduces the nuclear diameter of HeLa S3 cells. B. Bar graph represents HeLa S3 nuclei mean diameter after 5 minutes of UVC radiation with 30 J/m^2 in absence and presence of calcium chelators (EGTA and BAPTA-AM). (one-way ANOVA, *$p \leq 0.05$)

Figure 2.7: Calcium ions depletion impedes chromatin-dependent DNA protection from UV irradiation and impedes nucleotide excision repair Southwestern analysis of CPD and 6-4PP removal in the HeLa S3 cells. Cells were UVC irradiated with a dose of 30 J/m^2, 15J/m^2 , and twice 15 J/m^2 with 5 minutes break in presence and absence of EGTA and PABTA-AM. DNA was extracted from non-radiated cells and from cells immediately after irradiation, and 7 and 20 hours after irradiation for CPD, and DNA was extracted from non-radiated cells and from cells immediately after irradiation, and 2, 4 and 10 hours after irradiation. One µg of DNA was loaded per slot, on a slot blotter system and transferred to Hybond-N+ membrane. (A) The membranes were fixed at 80℃ for 15 minutes and incubated with anti-CPD monoclonal antibody, and (C) with 6-4PP monoclonal antibody. The CPDs and 6-4PP levels were standardized against the DNA levels by staining the membranes with ethidium bromide. (B) The percent of CPD/DNA (D) and 6-4PP/DNA were determined using densitometry of four independents CPD a 6-4PPs blots. The graphs represent the means (±SE) from three independent experiments. Note: The asterisks (*) indicated value that are significantly different between 30 J/m^2 with and without calcium chelators ($p \leq 0.05$) as determined by Kruskal-Wallis test.The double dragger (‡) indicated value that are significantly different between 15 J/m^2 with and without calcium chelator s ($p \leq 0.05$) as determined by Kruskal-Wallis test, $p > 0.05$.The number sign (#) indicated value that are significantly different between double 15 J/m^2 with and without calcium chelators ($p \leq 0.05$) as determined by Kruskal-Wallis test, $p \leq 0.05$.

Figure 1

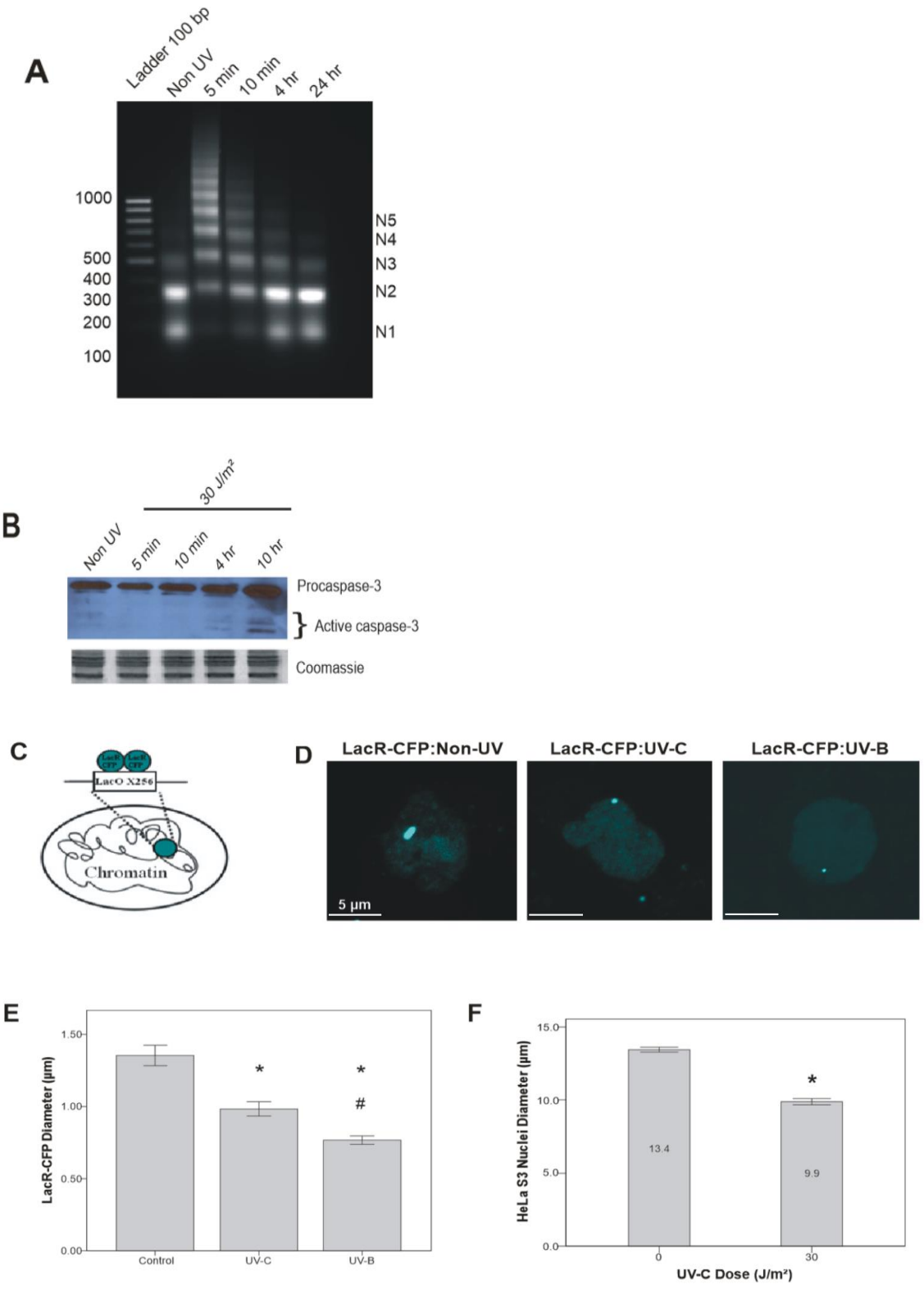
A
Ladder 100 bp
Non UV
5 min
10 min
4 hr
24 hr
1000
500
400
300
200
100
N5
N4
N3
N2
N1
B
30 J/m²
Non UV
5 min
10 min
4 hr
10 hr
Procaspase-3
Active caspase-3
Coomassie
C
LacO X256
Chromatin
D
LacR-CFP:Non-UV
LacR-CFP:UV-C
LacR-CFP:UV-B
5 µm
E
LacR-CFP Diameter (µm)
1.50
1.00
0.50
0.00
*
*
#
Control
UV-C
UV-B
F
HeLa S3 Nuclei Diameter (µm)
15.0
10.0
5.0
0.0
13.4
9.9
*
0
30
UV-C Dose (J/m²)

Figure 2

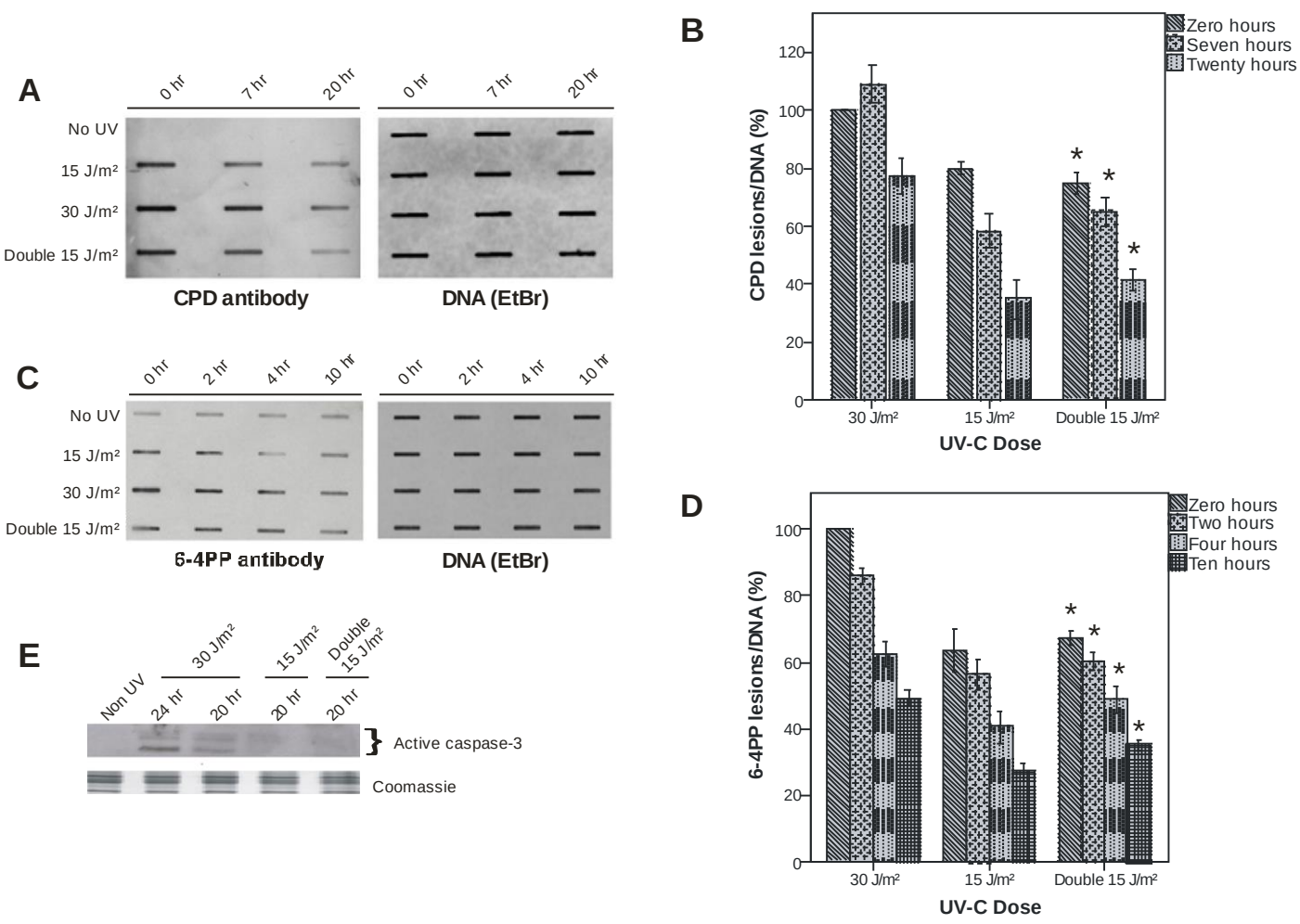
A
0 hr
7 hr
20 hr
No UV
15 J/m²
30 J/m²
Double 15 J/m²
CPD antibody
DNA (EtBr)
B
Zero hours
Seven hours
Twenty hours
CPD lesions/DNA (%)
UV-C Dose
30 J/m²
15 J/m²
Double 15 J/m²
C
2 hr
4 hr
10 hr
6-4PP antibody
D
Two hours
Four hours
Ten hours
6-4PP lesions/DNA (%)
E
Non UV
24 hr
Active caspase-3
Coomassie

Figure 4

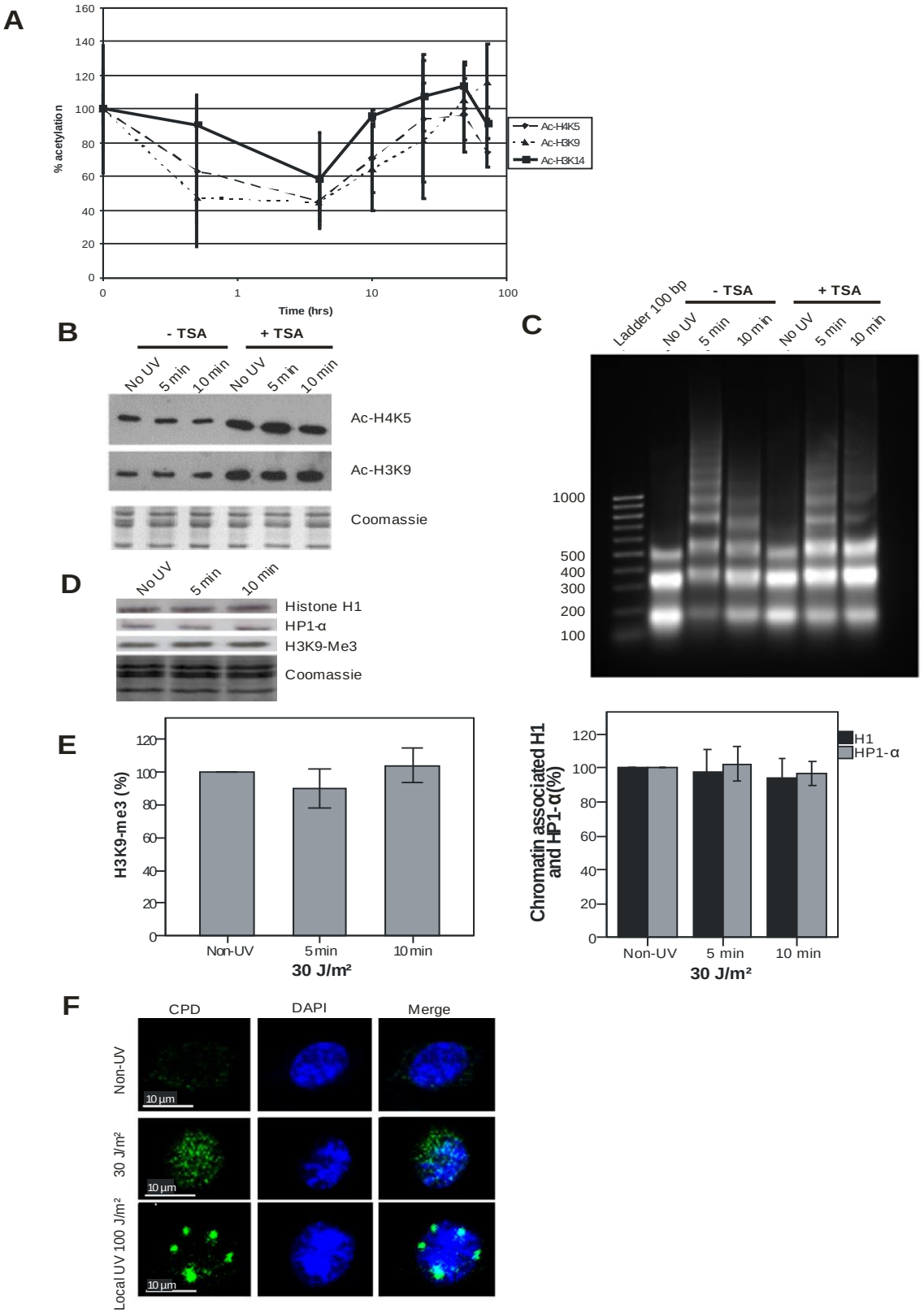
A
% acetylation
Time (hrs)
Ac-H4K5
Ac-H3K9
Ac-H3K14
B
- TSA
+ TSA
No UV
5 min
10 min
Ac-H4K5
Ac-H3K9
Coomassie
C
Ladder 100 bp
1000
500
400
300
200
100
D
Histone H1
HP1-α
H3K9-Me3
Coomassie
E
H3K9-me3 (%)
Non-UV
30 J/m²
Chromatin associated H1 and HP1-α(%)
H1
HP1-α
F
CPD
DAPI
Merge
Non-UV
30 J/m²
Local UV 100 J/m²
10 µm

Figure 5

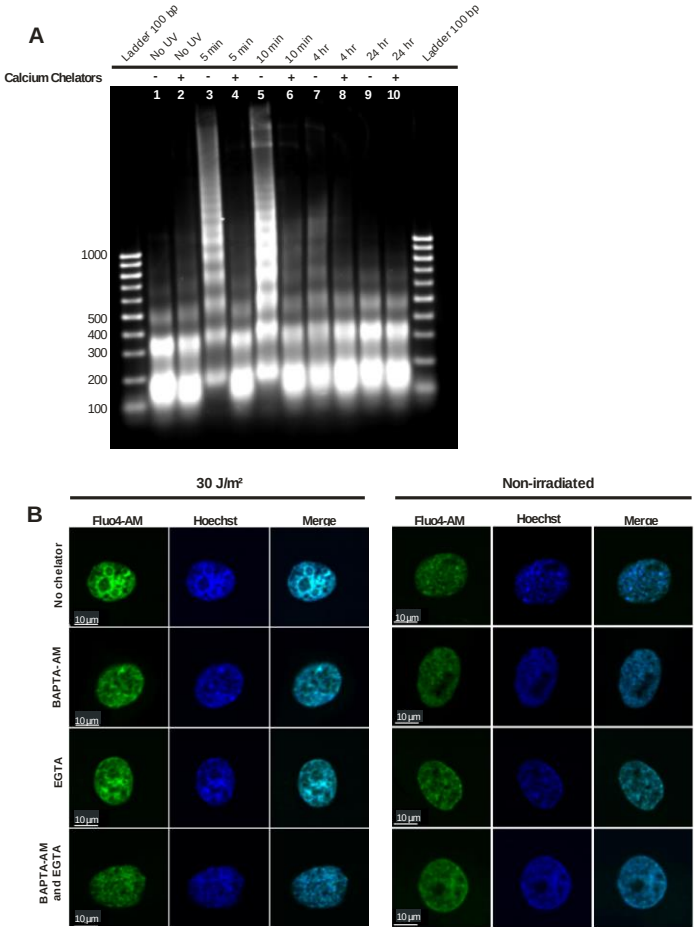
A
Ladder 100 bp
No UV
No UV
5 min
5 min
10 min
10 min
4 hr
4 hr
24 hr
24 hr
Ladder 100 bp
Calcium Chelators
- + - + - + - + - +
1 2 3 4 5 6 7 8 9 10
1000
500
400
300
200
100
B
30 J/m²
Non-irradiated
Fluo4-AM
Hoechst
Merge
Fluo4-AM
Hoechst
Merge
No chelator
BAPTA-AM
EGTA
BAPTA-AM and EGTA
10 µm

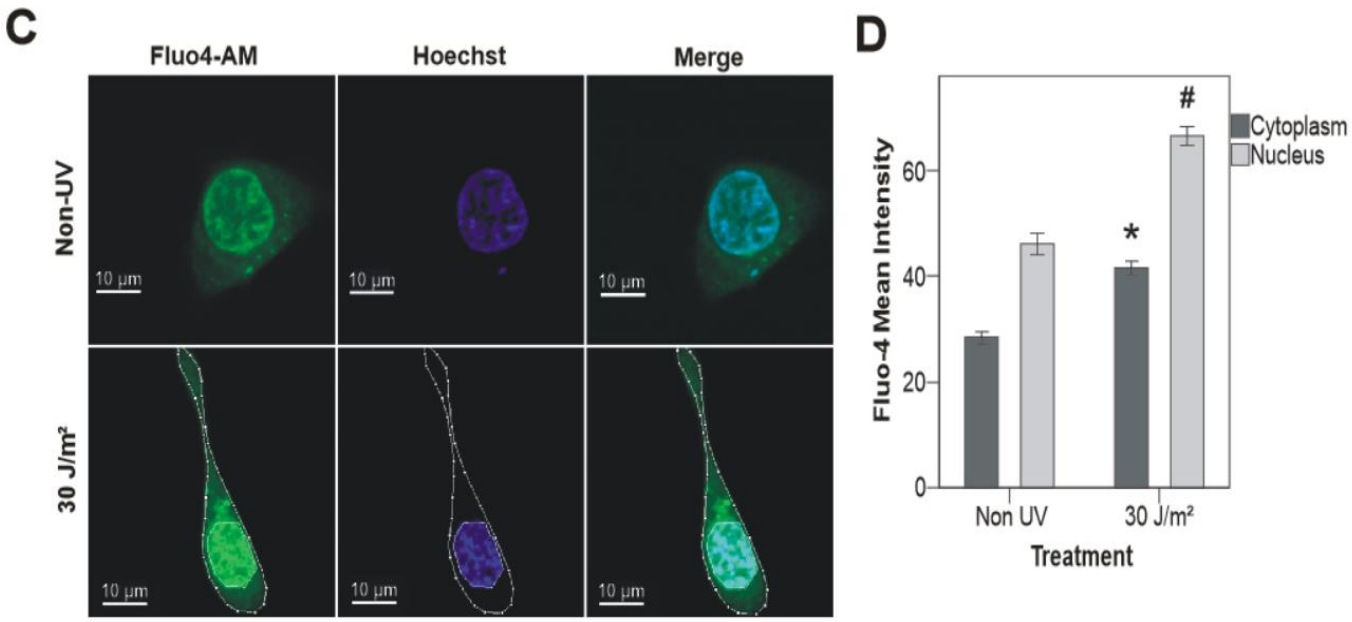
C
Fluo4-AM
Hoechst
Merge
Non-UV
30 J/m²
10 µm
D
Fluo-4 Mean Intensity
0
20
40
60
*
#
Non UV
30 J/m²
Treatment
Cytoplasm
Nucleus

Figure 6

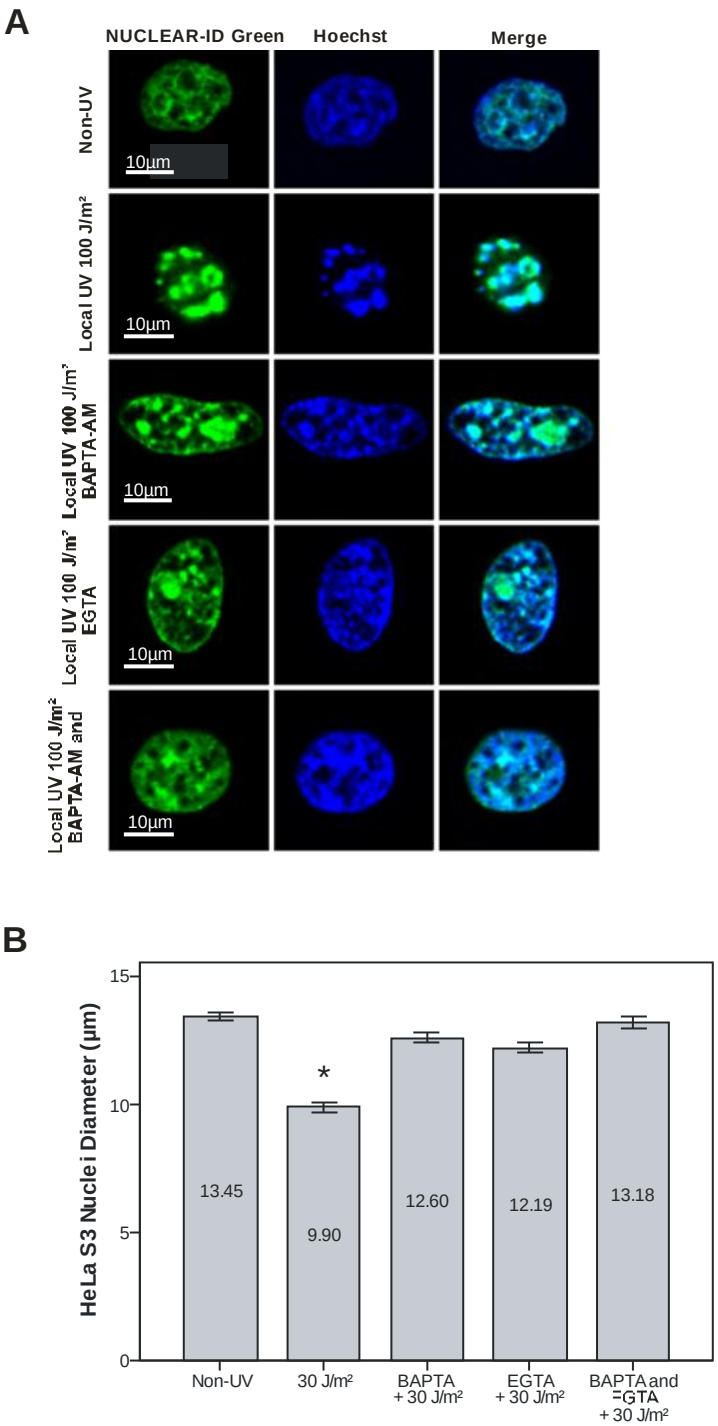
A
NUCLEAR-ID Green
Hoechst
Merge
Non-UV
Local UV 100 J/m²
Local UV 100 J/m² BAPTA-AM
Local UV 100 J/m² EGTA
Local UV 100 J/m² BAPTA-AM and EGTA
10µm
B
HeLa S3 Nuclei Diameter (µm)
15
10
5
0
13.45
9.90
12.60
12.19
13.18
*
Non-UV
30 J/m²
BAPTA + 30 J/m²
EGTA + 30 J/m²
BAPTA and EGTA + 30 J/m²

Figure 7

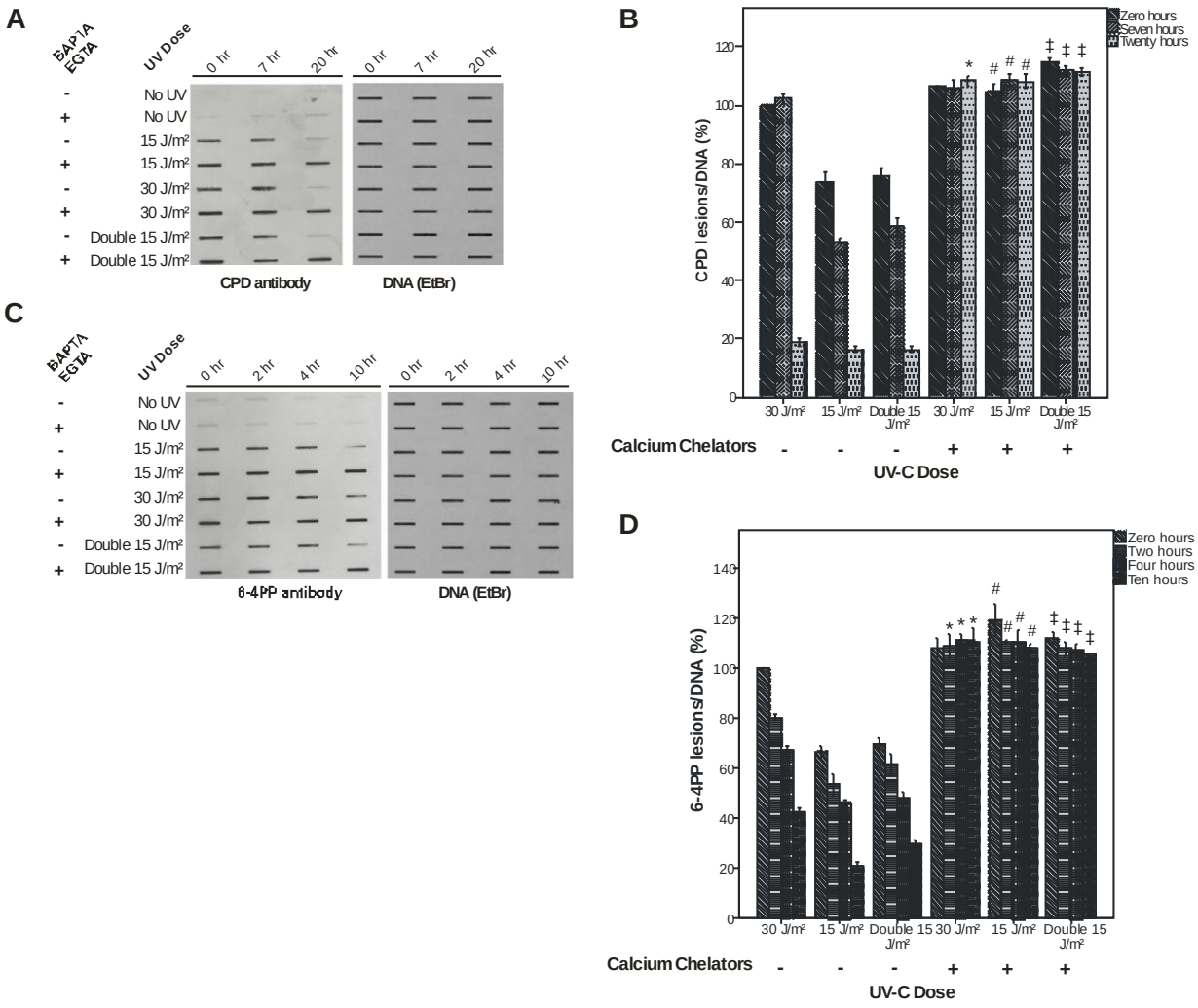
A
BAPTA EGTA
UV Dose
0 hr
7 hr
20 hr
No UV
15 J/m²
30 J/m²
Double 15 J/m²
CPD antibody
DNA (EtBr)
B
CPD lesions/DNA (%)
Zero hours
Seven hours
Twenty hours
30 J/m²
15 J/m²
Double 15 J/m²
Calcium Chelators
UV-C Dose
C
2 hr
4 hr
10 hr
6-4PP antibody
D
6-4PP lesions/DNA (%)
Zero hours
Two hours
Four hours
Ten hours

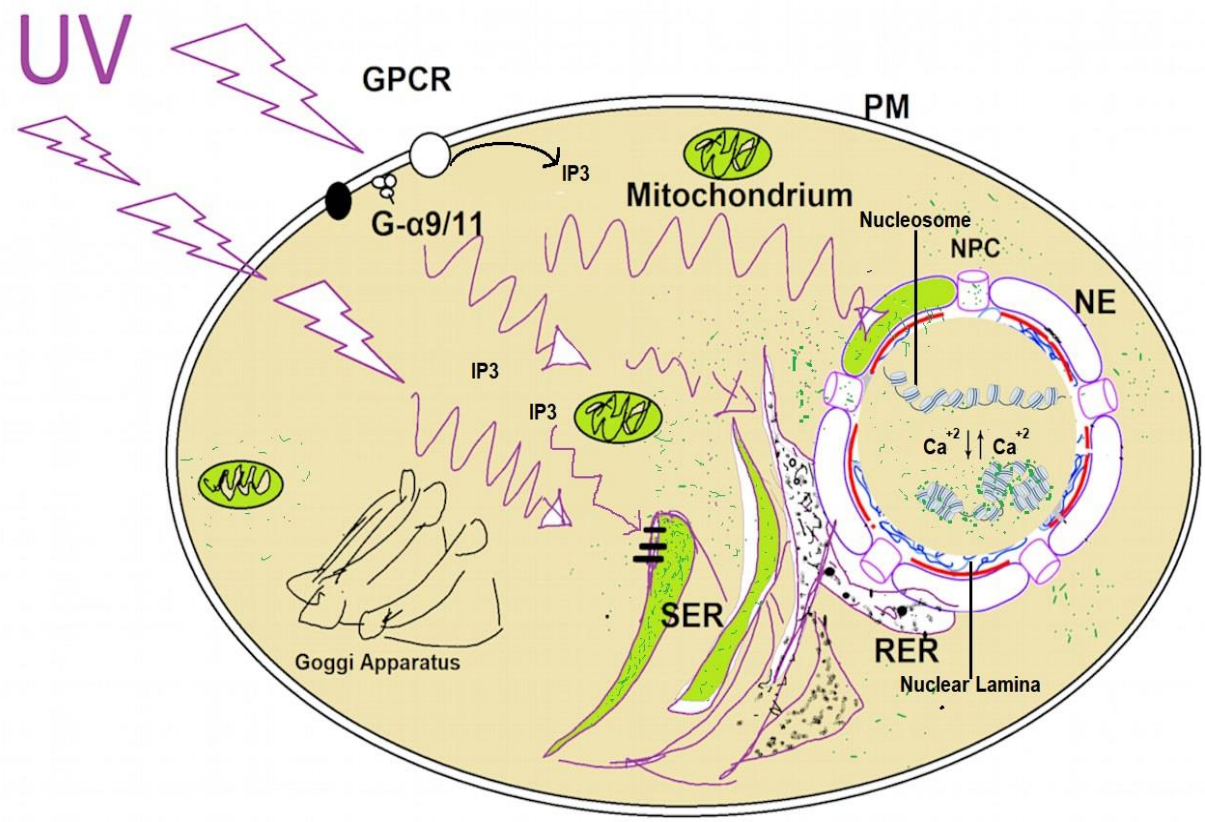

Figure (8). Chromatin Compaction mechanism suggested Model

References

Barnes, P.J., Adcock, I.M., and Ito, K. (2005). Histone acetylation and deacetylation: importance in inflammatory lung diseases. Eur Respir J *25*, 552-563.

Bedekovics, J., Irsai, G., Hegyi, K., Beke, L., Krenacs, L., Gergely, L., and Mehes, G. (2018). Mitotic Index Determined by Phosphohistone H3 Immunohistochemistry for Precise Grading in Follicular Lymphoma. Appl Immunohistochem Mol Morphol *26*, 579-585.

Bellono, N.W., Kammel, L.G., Zimmerman, A.L., and Oancea, E. (2013). UV light phototransduction activates transient receptor potential A1 ion channels in human melanocytes. Proc Natl Acad Sci U S A *110*, 2383-2388.

Cadet, J., Douki, T., Ravanat, J.L., and Di Mascio, P. (2009). Sensitized formation of oxidatively generated damage to cellular DNA by UVA radiation. Photochem Photobiol Sci *8*, 903-911.

Cann, K.L., and Dellaire, G. (2011). Heterochromatin and the DNA damage response: the need to relax. Biochem Cell Biol *89*, 45-60.

Chathoth, S., Thayyullathil, F., Hago, A., Shahin, A., Patel, M., and Galadari, S. (2009). UVC-induced apoptosis in Dubca cells is independent of JNK activation and p53(Ser-15) phosphorylation. Biochem Biophys Res Commun *383*, 426-432.

Dahle, J., and Kvam, E. (2003). Induction of delayed mutations and chromosomal instability in fibroblasts after UVA-, UVB-, and X-radiation. Cancer Res *63*, 1464-1469.

Dechat, T., Adam, S.A., and Goldman, R.D. (2009). Nuclear lamins and chromatin: when structure meets function. Adv Enzyme Regul *49*, 157-166.

Dillon, N. (2008). The impact of gene location in the nucleus on transcriptional regulation. Dev Cell *15*, 182-186.

Dinant, C., Bartek, J., and Bekker-Jensen, S. (2012). Histone displacement during nucleotide excision repair. Int J Mol Sci *13*, 13322-13337.

Douki, T., Bretonniere, Y., and Cadet, J. (2000). Protection against radiation-induced degradation of DNA bases by polyamines. Radiat Res *153*, 29-35.

Downing, K.H. (2000). Structural basis for the interaction of tubulin with proteins and drugs that affect microtubule dynamics. Annu Rev Cell Dev Biol *16*, 89-111.

Fraser, P., and Bickmore, W. (2007). Nuclear organization of the genome and the potential for gene regulation. Nature *447*, 413-417.

Friedberg, E.C. (2003). DNA damage and repair. Nature *421*, 436-440.

Friedberg, E.C., Aguilera, A., Gellert, M., Hanawalt, P.C., Hays, J.B., Lehmann, A.R., Lindahl, T., Lowndes, N., Sarasin, A., and Wood, R.D. (2006). DNA repair: from molecular mechanism to human disease. DNA Repair (Amst) *5*, 986-996.

Gan, H.H., and Schlick, T. (2010). Chromatin ionic atmosphere analyzed by a mesoscale electrostatic approach. Biophys J *99*, 2587-2596.

Goodsell, D.S. (2001). The molecular perspective: ultraviolet light and pyrimidine dimers. Oncologist *6*, 298-299.

Gospodinov, A., and Herceg, Z. (2013). Shaping chromatin for repair. Mutat Res *752*, 45-60.

Green, C.M., and Almouzni, G. (2002). When repair meets chromatin. First in series on chromatin dynamics. EMBO Rep *3*, 28-33.

Grigoryev, S.A., Arya, G., Correll, S., Woodcock, C.L., and Schlick, T. (2009). Evidence for heteromorphic chromatin fibers from analysis of nucleosome interactions. Proc Natl Acad Sci U S A *106*, 13317-13322.

Gross-Bellard, M., Oudet, P., and Chambon, P. (1973). Isolation of high-molecular-weight DNA from mammalian cells. Eur J Biochem *36*, 32-38.

Hamilton, C., Hayward, R.L., and Gilbert, N. (2011). Global chromatin fibre compaction in response to DNA damage. Biochem Biophys Res Commun *414*, 820-825.

Hergeth, S.P., and Schneider, R. (2015). The H1 linker histones: multifunctional proteins beyond the nucleosomal core particle. EMBO Rep *16*, 1439-1453.

Herrling, T., Jung, K., and Fuchs, J. (2006). Measurements of UV-generated free radicals/reactive oxygen species (ROS) in skin. Spectrochim Acta A Mol Biomol Spectrosc *63*, 840-845.

Hihara, S., Pack, C.G., Kaizu, K., Tani, T., Hanafusa, T., Nozaki, T., Takemoto, S., Yoshimi, T., Yokota, H., Imamoto, N.*, et al.* (2012). Local nucleosome dynamics facilitate chromatin accessibility in living mammalian cells. Cell Rep *2*, 1645-1656.

Hochberg, M., Kohen, R., and Enk, C.D. (2006). Role of antioxidants in prevention of pyrimidine dimer formation in UVB irradiated human HaCaT keratinocytes. Biomed Pharmacother *60*, 233-237.

Imai, S., Johnson, F.B., Marciniak, R.A., McVey, M., Park, P.U., and Guarente, L. (2000). Sir2: an NAD-dependent histone deacetylase that connects chromatin silencing, metabolism, and aging. Cold Spring Harb Symp Quant Biol *65*, 297-302.

Jordan, M.A., and Wilson, L. (1998). Microtubules and actin filaments: dynamic targets for cancer chemotherapy. Curr Opin Cell Biol *10*, 123-130.

Kahl, C.R., and Means, A.R. (2003). Regulation of cell cycle progression by calcium/calmodulin-dependent pathways. Endocr Rev *24*, 719-736.

Kalverda, B., Roling, M.D., and Fornerod, M. (2008). Chromatin organization in relation to the nuclear periphery. FEBS Lett *582*, 2017-2022.

Kornberg, R.D., and Lorch, Y. (1999a). Chromatin-modifying and -remodeling complexes. Curr Opin Genet Dev *9*, 148-151.

Kornberg, R.D., and Lorch, Y. (1999b). Twenty-five years of the nucleosome, fundamental particle of the eukaryote chromosome. Cell *98*, 285-294.

Korolev, N., Allahverdi, A., Yang, Y., Fan, Y., Lyubartsev, A.P., and Nordenskiold, L. (2010). Electrostatic origin of salt-induced nucleosome array compaction. Biophys J *99*, 1896-1905.

Korolev, N., Zhao, Y., Allahverdi, A., Eom, K.D., Tam, J.P., and Nordenskiold, L. (2012). The effect of salt on oligocation-induced chromatin condensation. Biochem Biophys Res Commun *418*, 205-210.

Kulms, D., and Schwarz, T. (2000). Molecular mechanisms of UV-induced apoptosis. Photodermatol Photoimmunol Photomed *16*, 195-201.

Lachner, M., O'Carroll, D., Rea, S., Mechtler, K., and Jenuwein, T. (2001). Methylation of histone H3 lysine 9 creates a binding site for HP1 proteins. Nature *410*, 116-120.

Lin, J., Chen, F., Sun, M.J., Zhu, J., Li, Y.W., Pan, L.Z., Zhang, J., and Tan, J.H. (2016). The relationship between apoptosis, chromatin configuration, histone modification and competence of oocytes: A study using the mouse ovary-holding stress model. Sci Rep *6*, 28347.

Mateos-Langerak, J., Goetze, S., Leonhardt, H., Cremer, T., van Driel, R., and Lanctot, C. (2007). Nuclear architecture: Is it important for genome function and can we prove it? J Cell Biochem *102*, 1067-1075.

Misteli, T. (2007). Beyond the sequence: cellular organization of genome function. Cell *128*, 787-800.

Miyamura, Y., Coelho, S.G., Wolber, R., Miller, S.A., Wakamatsu, K., Zmudzka, B.Z., Ito, S., Smuda, C., Passeron, T., Choi, W.*, et al.* (2007). Regulation of human skin pigmentation and responses to ultraviolet radiation. Pigment Cell Res *20*, 2-13.

Moan, J., Nielsen, K.P., and Juzeniene, A. (2012). Immediate pigment darkening: its evolutionary roles may include protection against folate photosensitization. FASEB J *26*, 971-975.

Nielsen, A.L., Oulad-Abdelghani, M., Ortiz, J.A., Remboutsika, E., Chambon, P., and Losson, R. (2001). Heterochromatin formation in mammalian cells: interaction between histones and HP1 proteins. Mol Cell *7*, 729-739.

Pillai, S., Oresajo, C., and Hayward, J. (2005). Ultraviolet radiation and skin aging: roles of reactive oxygen species, inflammation and protease activation, and strategies for prevention of inflammation-induced matrix degradation - a review. Int J Cosmet Sci *27*, 17-34.

Polo, S.E., and Almouzni, G. (2015). Chromatin dynamics after DNA damage: The legacy of the access-repair-restore model. DNA Repair (Amst) *36*, 114-121.

Rastogi, R.P., Richa, Kumar, A., Tyagi, M.B., and Sinha, R.P. (2010). Molecular mechanisms of ultraviolet radiation-induced DNA damage and repair. J Nucleic Acids *2010*, 592980.

Roque, A., Ponte, I., and Suau, P. (2016). Interplay between histone H1 structure and function. Biochim Biophys Acta *1859*, 444-454.

Ruan, K., Yamamoto, T.G., Asakawa, H., Chikashige, Y., Kimura, H., Masukata, H., Haraguchi, T., and Hiraoka, Y. (2015). Histone H4 acetylation required for chromatin decompaction during DNA replication. Sci Rep *5*, 12720.

Schlick, T., Hayes, J., and Grigoryev, S. (2012). Toward convergence of experimental studies and theoretical modeling of the chromatin fiber. J Biol Chem *287*, 5183-5191.

Schmitges, F.W., Prusty, A.B., Faty, M., Stutzer, A., Lingaraju, G.M., Aiwazian, J., Sack, R., Hess, D., Li, L., Zhou, S.*, et al.* (2011). Histone methylation by PRC2 is inhibited by active chromatin marks. Mol Cell *42*, 330-341.

Schwarz, A., Stander, S., Berneburg, M., Bohm, M., Kulms, D., van Steeg, H., Grosse-Heitmeyer, K., Krutmann, J., and Schwarz, T. (2002). Interleukin-12 suppresses ultraviolet radiation-induced apoptosis by inducing DNA repair. Nat Cell Biol *4*, 26-31.

Skelding, K.A., Rostas, J.A., and Verrills, N.M. (2011). Controlling the cell cycle: the role of calcium/calmodulin-stimulated protein kinases I and II. Cell Cycle *10*, 631-639.

Smith, K.T., and Workman, J.L. (2012). Chromatin proteins: key responders to stress. PLoS Biol *10*, e1001371.

Soria, G., Polo, S.E., and Almouzni, G. (2012). Prime, repair, restore: the active role of chromatin in the DNA damage response. Mol Cell *46*, 722-734.

Soutoglou, E., and Misteli, T. (2008). Activation of the cellular DNA damage response in the absence of DNA lesions. Science *320*, 1507-1510.

Spotheim-Maurizot, M., Ruiz, S., Sabattier, R., and Charlier, M. (1995). Radioprotection of DNA by polyamines. Int J Radiat Biol *68*, 571-577.

Strayer, D.S., Hoek, J.B., Thomas, A.P., and White, M.K. (1999). Cellular activation by Ca2+ release from stores in the endoplasmic reticulum but not by increased free Ca2+ in the cytosol. Biochem J *344 Pt 1*, 39-46.

Strick, R., Strissel, P.L., Gavrilov, K., and Levi-Setti, R. (2001). Cation-chromatin binding as shown by ion microscopy is essential for the structural integrity of chromosomes. J Cell Biol *155*, 899-910.

Suzuki, K., Yamauchi, M., Oka, Y., Suzuki, M., and Yamashita, S. (2010). A novel and simple micro-irradiation technique for creating localized DNA double-strand breaks. Nucleic Acids Res *38*, e129.

Takata, H., Hanafusa, T., Mori, T., Shimura, M., Iida, Y., Ishikawa, K., Yoshikawa, K., Yoshikawa, Y., and Maeshima, K. (2013). Chromatin compaction protects genomic DNA from radiation damage. PLoS One *8*, e75622.

Tan, R., and Lan, L. (2016). Guarding chromosomes from oxidative DNA damage to the very end. Acta Biochim Biophys Sin (Shanghai) *48*, 617-622.

Tombes, R.M., and Borisy, G.G. (1989). Intracellular free calcium and mitosis in mammalian cells: anaphase onset is calcium modulated, but is not triggered by a brief transient. J Cell Biol *109*, 627-636.

Trinkle-Mulcahy, L., and Lamond, A.I. (2008). Nuclear functions in space and time: gene expression in a dynamic, constrained environment. FEBS Lett *582*, 1960-1970.

Tumbar, T., Sudlow, G., and Belmont, A.S. (1999). Large-scale chromatin unfolding and remodeling induced by VP16 acidic activation domain. J Cell Biol *145*, 1341-1354.

Vanhaecke, T., Papeleu, P., Elaut, G., and Rogiers, V. (2004). Trichostatin A-like hydroxamate histone deacetylase inhibitors as therapeutic agents: toxicological point of view. Curr Med Chem *11*, 1629-1643.

Warters, R.L., Newton, G.L., Olive, P.L., and Fahey, R.C. (1999). Radioprotection of human cell nuclear DNA by polyamines: radiosensitivity of chromatin is influenced by tightly bound spermine. Radiat Res *151*, 354-362.

Wasmeier, C., Hume, A.N., Bolasco, G., and Seabra, M.C. (2008). Melanosomes at a glance. J Cell Sci *121*, 3995-3999.

Wicks, N.L., Chan, J.W., Najera, J.A., Ciriello, J.M., and Oancea, E. (2011). UVA phototransduction drives early melanin synthesis in human melanocytes. Curr Biol *21*, 1906-1911.

Zeng, W., Ball, A.R., Jr., and Yokomori, K. (2010). HP1: heterochromatin binding proteins working the genome. Epigenetics *5*, 287-292.

CHAPTER III

Results

Local UV-induced chromatin compaction is photolesions site-independent.

To study if the chromatin compaction takes place just on the site of photoproducts or globally, we used local UV irradiation and immunofluorescence microscopy (Suzuki et al., 2010). The UV irradiation of the cells was done locally at 100 J/m^2 through an isopore polycarbonate membrane filter (3 µm in size), which generated damage in a spotted pattern. Cells were incubated for different time points and then fixed and then incubated with antibodies against CPD and stained with Hoechst as a counterstain (Figure 1). Local UV irradiation results showed that chromatin compaction is not colocalized with areas of UV damage the (CPD foci).

Calcium chelator BAPTA-AM reduces the chromatin compaction upon UV irradiation.

The NUCLEAR-ID Green chromatin condensation detection kit was used to stain the condensed chromatin. HeLa cells were plated in clear bottom 96-well plates and treated with BAPTA-AM and then UV-irradiated with 70 J/m^2. Cells that were not irradiated and not treated with Ca^{2+}-chelating agents BAPTA-AM served as negative controls. Microplate reader with excitation wavelength 488nm and emission wavelength 520nm was used to measure fluorescent signals for three independent experiments (Figure 2). When the cells were irradiated, we observed significantly higher fluorescent signals intensity compared to the unirradiated cells. However, when the cells treated

with chelating agent, there was a significant reduction in the fluorescent signal intensity, which means less chromatin compaction.

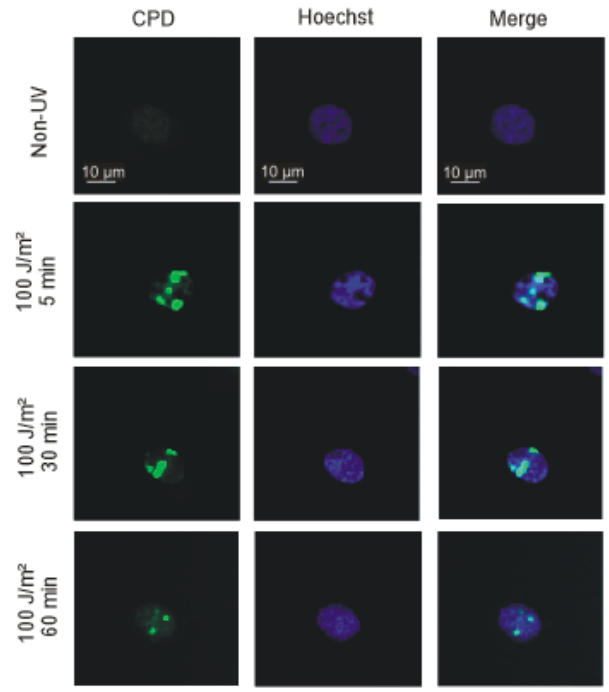

Figure 3.1: Detection of locally induced UV damage in cell nuclei. A UV-blocking polycarbonate filter containing pores of 3 µm in diameter was used to cover a monolayer of cells. The filter-covered cells were UV irradiated with 100 J/m^2 and, cells were incubated for 5 minutes, 30 minutes, and 60 minutes and then then fixed. CPDs were tagged anti-CPD antibodies followed by secondary fluorescently conjugated-antibodies directed against the primary antibodies. Nuclei were counter-stained with Hoechst staining.

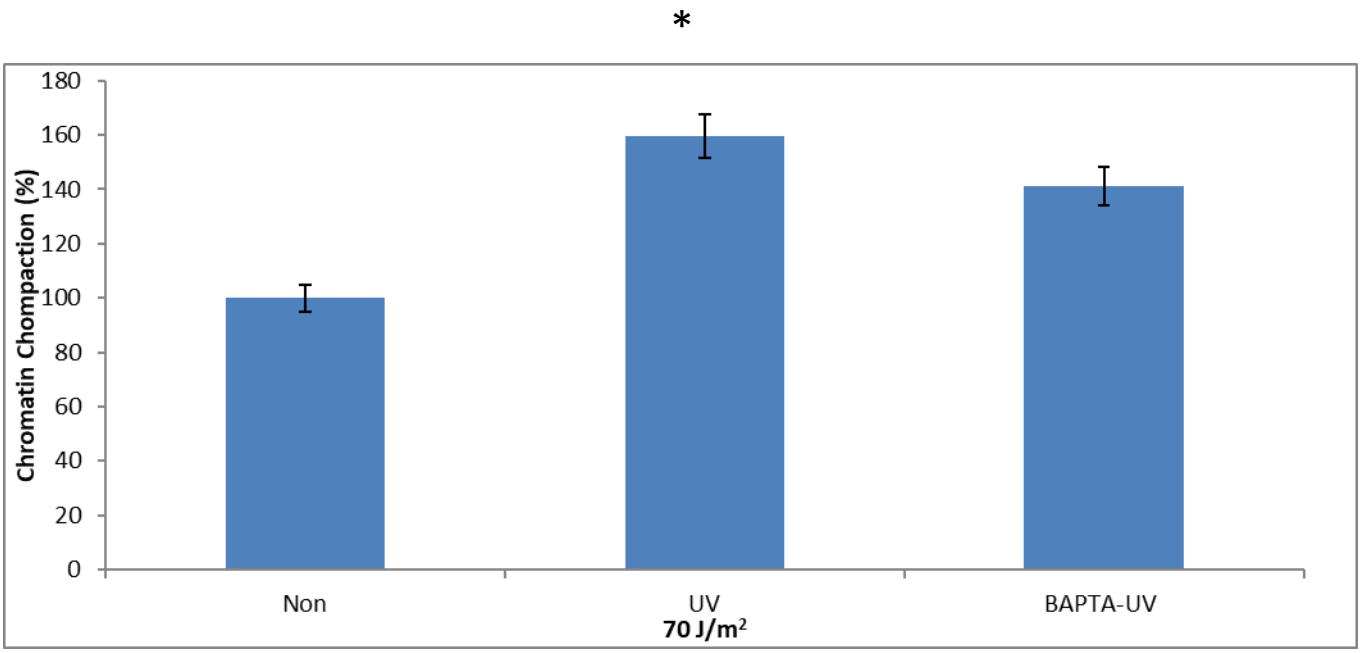

Figure 3.2 Calcium chelators reduce chromatin compaction after UV irradiation. NUCLEAR-ID green chromatin condensation detection kit was used to analyze chromatin condensation using a fluorescence microplate reader. HeLa cells were plated in 96-well plates, treated with BAPTA-AM and then UV-irradiated with 70 J/m^2. Fluorescent signals are in relative fluorescence Units (RFUs) and linearity was verified with appropriate filter sets according to instrument specifications.

CHAPTER IV

Discussion

In this study, we used micrococcal nuclease assay, fluorescent microscopy, and southwestern techniques to analyze the effect of ultraviolet C light irradiation on the compaction level of chromatin in HeLa cells and within the nuclei of mouse fibroblast NIH2/4 cells. Over the past few decades, studies have shown the cellular response that follows DNA damage, termed DNA damage response (DDR) is accompanied by changes in chromatin structure (Carrier et al., 1999; Ciccia and Elledge, 2010; Ziv et al., 2006). Studies suggested that upon damage, chromatin unfolds around the lesions by the action of chromatin remodeling factors and histone-modifying enzymes. Once DNA is accessible to enable DNA repair, DNA repair takes place and it is followed by restoration of chromatin to the pre-lession steady state involving histone chaperones and remodeling factors (Luijsterburg and van Attikum, 2011; Ransom et al., 2010; Soria et al., 2012). Unlike the presumptive three-step model that describes the site of DNA damage and repair in the context of chromatin—access, repair and restore (ARR) model, our findings in this study indicate that on a global scale, the chromatin is condensed immediately after UV irradiation. We also showed that the chromatin condensation after UV irradiation is independent of histones modifications such as acetylation and known chromatin condensing proteins such as H1 and HP1. We demonstrated that chromatin compaction is strongly affected by calcium cation influx following UV irradiation, which mediates the global chromatin compaction. This

mechanism appears to be part of a physiological response that protects from further DNA damage.

Micrococcal nuclease digestion of UV irradiated HeLa cells showed a decrease in chromatin sensitivity to micrococcal nuclease as a result of immediate chromatin compaction five minutes after UV-irradiation. Twenty-four hours after irradiation, the chromatin returned to the pre-UV steady-state compaction level. NIH2/4 cells also showed chromatin compaction instantaneously after UVB and UVC irradiation. NIH2/4 are stably transfected with an array of 256 repeats of Lac operon sequence (LacO) that can bind multiple copies of Lac repressor (LacR) fused to CFP (LacR-CFP). Fusion proteins containing the LacR-CFP are tethered to the LacO sites, inducing small compacted dot in the nucleus of the cells that can be visualized in living cells (Soutoglou and Misteli, 2008; Tumbar et al., 1999). Diameters of the specs marking the chromatin domain of fusion proteins LacO:LacR-CFP showed a significant condensation after UV irradiation. These results combined suggest that there is a global UV effect which compact chromatin although this does not exclude the report by others that chromatin can locally detect and respond to sites of DNA damage. It has been shown that chromatin undergoes condensation after lethal genotoxic treatment such as UV radiations as part of the apoptotic process (Farkas et al., 2010; Lane et al., 2005). Apoptosis analysis by the apoptosis marker active caspase-3 after UV irradiation, did not suggest that apoptotic effects take part in the cell in the first hour after UV-irradiation. Thus, this chromatin compaction is not due to apoptotic bodies, formation after UV-irradiation.

The two main UV-induced photoproducts, CPDs, and 6-4PPs, are not similarly detected in the nucleus of UV-irradiated cells and are produced in distinct locations of the chromatin (Pfeifer, 1997). Indeed, they are generated in different amounts; they do not distort the double helix at the same degree and since 6-4PPs create more distortion, radiated cells required less time to detect and repair 6-4PPs via nucleotide excision repair (NER) (Bergink et al., 2006; Sage, 1993).

First and foremost, we suggested that the chromatin undergoes into a higher compaction state after UV-irradiation possibly to protect from further DNA-damage. To better understand the effect of chromatin condensation on DNA protection, we established a new assay using double UV irradiation principle. The UV induced photoproducts CPDs and 6-4PPs were analyzed globally in irradiated HeLa cells. Moreover, we used synchronized cells at mitotic stages to test and determine if the condensed mitotic chromatin provides natural protective barrier that suppress further DNA damage. Undoubtedly, synchronized mitotic chromatin irradiation showed more protection against photolesions than the non-mitotic chromatin. Cells that were double irradiated at 15 J/m^2 with five minutes break had significantly lower cyclobutane pyrimidine dimer (CPD) and 6-4 photoproduct (6-4PP) rates in comparison to cells subjected to 30 J/m^2. It has been suggested in many studies that ultraviolet light induces free radical formation in skin cells and indirectly contribute to CPD formation (Hochberg et al., 2006; Jurkiewicz and Buettner, 1994). We believe that the increase in CPDs not 6-4PPs level after UV irradiation is affected by the level of free radicals produced after UV radiation.

Additionally, by using different UV intensities that delivered the same dose but in a shorter or a longer time and then measuring the rate of photolesion removal over time, we further supported the notion that the chromatin compaction and protection is a coupled process that happens simultaneously. The next question was: What is the molecular mechanism that causes this instant compaction? Histones' post-translational modifications have the potential to directly modulate nucleosome structure and consequently chromatin structure and DNA accessibility (Bannister and Kouzarides, 2011). Indeed, the acetylation state of histone tail lysine residues regulates both the local chromatin dynamics as well as the higher-order chromatin structure (Schneider and Grosschedl, 2007).

It is documented that histone H3 and histone H4 acetylation both disrupts the formation of higher-order chromatin structure and changes the functional interaction of chromatin-associated proteins, thereby increasing chromatin accessibility and vice-versa (Hunt et al., 2013; Shogren-Knaak et al., 2006). Furthermore, previous studies have shown hyperacetylation of histone H3 Lysine 9 (H3-K9ac), and lysine 14 (H3-K14ac) following UV irradiation of yeast cells and mouse embryonic fibroblasts (MEF cells) (Lange et al., 2008; Yu et al., 2005). Hyperacetylation events occurred 30 minutes immediately after UV irradiation, and level hyperacetylation diminished progressively as repair proceeded (Yu et al., 2005).

On the contrary, our results showed a wave of global deacetylation of histone H3 on Lysine 9 (H3-K9ac), lysine 14 (H3-K14ac), and H4 on lysine 5 (H4-K5ac) that peaked 4 hours after UV irradiation and chromatin condensation in human Hela cells. A global

wave of deacetylation of histone H3-K9ac and H3-K56 in response to UV irradiation and other stress was shown in a different study (Tjeertes et al., 2009).

Histone deacetylases (HDAC) and histone acetyltransferases control the acetylation state of lysine residues, including those situated in the N-terminal 'tails' of histones. HDAC inhibitors (HDACis) comprise a diverse range of unrelated compounds that all induce an accumulation of hyperacetylated histones resulting in various biological effects. Trichostatin A (TSA) is an HDAC inhibitor, and incubation with TSA and then UV irradiating HeLa cells is expected to show hyperacetylation of histone H3 on Lysine 9 (H3-K9ac), and H4 on lysine 5 (H4-K5ac). Conducting this experiment would reveal whether the deacetylation of the core histones is required for the compaction of chromatin following UV radiation. Micrococcal nuclease digestion of TSA treated and UV irradiated HeLa cells showed the same results as TSA untreated and UV irradiated cells with a nonsignificant increase in chromatin sensitivity to micrococcal nuclease in the TSA treated cells. However, a similar pattern of digestion and the same level of compactness were observed.

Linker histone H1 (H1) is known to be a key protein involved chromatin condensation in vivo (Allan et al., 1980; Bharath et al., 2002; Hendzel et al., 2004). The linker histone H1 is a component of chromatin and binds to the nucleosomal core particle around the DNA entry and exit sites and the linker DNA. H1 can stabilize both nucleosome structure and higher-order chromatin architecture in both euchromatin and heterochromatin. In general, H1 molecules consist of a central globular domain and a

more flexible tail regions at both their N- and C-terminal ends (Bustin et al., 2005; Hergeth and Schneider, 2015; Roque et al., 2005).

Another highly conserved chromatin-binding protein named heterochromatin protein 1 (HP1) or its orthologue exists in organisms ranging from yeast to human (Zeng et al., 2010). HP1 also plays a critical role in higher-order chromatin architecture in which its amino-terminal chromodomain binds methylated lysine 9 of histone H3, causing transcriptional repression. The highly conserved carboxy-terminal domain of HP1 enables dimerization also serves as a docking site for proteins involved in a wide variety of nuclear functions, from transcription to nuclear architecture. In addition to heterochromatin packaging, it is becoming increasingly clear that HP1 proteins have diverse roles in the nucleus, including the regulation of euchromatic genes (Lomberk et al., 2006; Norwood et al., 2004; Tombes and Borisy, 1989). However, our results in this work suggest that linker histone H1 and Heterochromatin protein 1- α do not contribute to chromatin compaction after UV irradiation since they were found to be associated with chromatin at the same level before and after UV-irradiation.

The conclusion from these experiment is that chromatin compaction upon UV irradiation is not dependent on epigenetic modifications and structural proteins. Mg^{2+} and Ca^{2+}, are known to increase and shift from their storage organelles to chromatin during the mitotic phase of the cell cycle (Strick et al., 2001; Tombes and Borisy, 1989). Furthermore, EM studies found that salt concentration is a crucial parameter for the formation of compacted chromatin 30 nm fibers, by using extracted chromosomes, monovalent (Na^{+} and K^{+}) and divalent (Mg^{2+} and Ca^{2+}) cations were identified as important factors

for controlling overall chromosome folding (Finch and Klug, 1976; Pruitt and Grainger, 1980; Widom, 1986; Woodcock et al., 1984).

In vitro analysis of reconstituted nucleosome arrays showed cation-dependent compaction with monovalent and divalent cations, and polyamine (Grigoryev et al., 2009; Hansen, 2002; Korolev et al., 2010). Positively charged ions neutralize the repulsion between the negatively charged DNA, thereby enhancing *in vitro* chromatin compaction. Other in-vitro studies revealed transitions in nucleosome folding status depending on calcium and magnesium concentration (Hansen, 2002; Maeshima et al., 2016; Robinson et al., 2006; Visvanathan et al., 2013). In micrococcal nuclease digestion of HeLa cells that were incubated with calcium chelators such as BAPTA-AM and EGTA did not show any change in chromatin sensitivity to micrococcal nuclease five and ten minutes after UV-irradiation. These results strongly suggest that calcium is an essential cation in chromatin compaction after UV irradiation. A couple of studies indicated that UVR phototransduction leads to activation of G- protein ($G\alpha_{9/11}$ subunit), which in turn activates phospholipase C β (PLCβ) activity which was required both for intracellular Ca^{2+} release and transient receptor potential A1 (TRPA1) activation in primary human melanocytes (Bellono et al., 2013; Wicks et al., 2011). In our work, microscopic studies of cellular and nuclear calcium levels in HeLa cells after UV irradiation revealed an immediate increased in intracellular and nuclear calcium cation.

Our findings demonstrated that Ca^{2+} is essential for the organization of a compacted chromatin level upon UV irradiation. We were able to detect a significant decrease in the HeLa cells' diameter upon UV irradiation. HeLa cells nuclei diameter reduction upon UV irradiation can be explained by the fact that nuclear lamins directly or indirectly

involved in anchoring chromatin to the nuclear lamina, which also acts as a nucleoplasmic scaffold for organizing chromatin in the nucleus (Bouvier et al., 1985; Mattout-Drubezki and Gruenbaum, 2003; Schirmer and Foisner, 2007; Takata et al., 2007). Based on our model, calcium influx in nuclei neutralized the negatively charged DNA phosphate groups, which led to chromatin compaction, and in turn this response caused pulling the nuclear envelope, which resulted in nuclear diameter and volume reduction.

We were unable to detect any significant change in HeLa cells nuclei upon UV-irradiation that were incubated with calcium chelators such as BAPTA-AM and EGTA separately or together which supported the causative role of calcium influx in UV-induced chromatin compaction. In our hypothesis about the role of calcium influx to nuclei is correct, we would expect the local UV irradiation of some regions in the nucleus would result in general chromatin compaction, which would not be confined to the irradiated foci. We used a method that produces UV-induced DNA damage within localized areas of the cell nucleus and allows us to subsequently visualize them *in situ*. Indeed, CPDs were produced and visualized as several foci per nucleus, and chromatin condensation appeared as an irregular spotty pattern, but there was no localization between CPDs distribution and chromatin compacted spots. Indeed, this finding supported the role of calcium influx, causing chromatin compaction.

Calcium depletion showed a considerable reduction in the size of condensed spotty chromatin. Besides employing southwestern blot analysis, we found that the cells that treated with calcium chelators and then irradiated had no DNA protection at all, and the nucleotide excision repair was disrupted as well. Since UV-damaged DNA-binding

protein-1 (UV-DDB1), which is part of NER has calcium-dependent DNA binding (He et al., 2006), chelating calcium resulting in an impaired removal rate of both CPDs and 6-4PPs.

Despite the ability of divalent calcium cations to promote chromatin condensation upon UV irradiation, we cannot rule out the involvement of other bivalent or polyvalent cations in the compaction of chromatin after UV irradiation.

References

Allan, J., Hartman, P.G., Crane-Robinson, C., and Aviles, F.X. (1980). The structure of histone H1 and its location in chromatin. Nature *288*, 675-679.

Andressoo, J.O., Hoeijmakers, J.H., and Mitchell, J.R. (2006). Nucleotide excision repair disorders and the balance between cancer and aging. Cell cycle *5*, 2886-2888.

Anna, B., Blazej, Z., Jacqueline, G., Andrew, C.J., Jeffrey, R., and Andrzej, S. (2007). Mechanism of UV-related carcinogenesis and its contribution to nevi/melanoma. Expert Rev Dermatol *2*, 451-469.

Bannister, A.J., and Kouzarides, T. (2011). Regulation of chromatin by histone modifications. Cell Res *21*, 381-395.

Barnes, P.J., Adcock, I.M., and Ito, K. (2005). Histone acetylation and deacetylation: importance in inflammatory lung diseases. Eur Respir J *25*, 552-563.

Beattie, P.E., Dawe, R.S., Ferguson, J., and Ibbotson, S.H. (2005). Dose-response and time-course characteristics of UV-A1 erythema. Arch Dermatol *141*, 1549-1555.

Bedekovics, J., Irsai, G., Hegyi, K., Beke, L., Krenacs, L., Gergely, L., and Mehes, G. (2018). Mitotic Index Determined by Phosphohistone H3 Immunohistochemistry for Precise Grading in Follicular Lymphoma. Appl Immunohistochem Mol Morphol *26*, 579-585.

Bellono, N.W., Kammel, L.G., Zimmerman, A.L., and Oancea, E. (2013). UV light phototransduction activates transient receptor potential A1 ion channels in human melanocytes. Proc Natl Acad Sci U S A *110*, 2383-2388.

Bergink, S., Salomons, F.A., Hoogstraten, D., Groothuis, T.A., de Waard, H., Wu, J., Yuan, L., Citterio, E., Houtsmuller, A.B., Neefjes, J.*, et al.* (2006). DNA damage triggers nucleotide excision repair-dependent monoubiquitylation of histone H2A. Genes Dev *20*, 1343-1352.

Bharath, M.M., Ramesh, S., Chandra, N.R., and Rao, M.R. (2002). Identification of a 34 amino acid stretch within the C-terminus of histone H1 as the DNA-condensing domain by site-directed mutagenesis. Biochemistry *41*, 7617-7627.

Bivik, C.A., Larsson, P.K., Kagedal, K.M., Rosdahl, I.K., and Ollinger, K.M. (2006). UVA/B-induced apoptosis in human melanocytes involves translocation of cathepsins and Bcl-2 family members. J Invest Dermatol *126*, 1119-1127.

Bohm, M., Wolff, I., Scholzen, T.E., Robinson, S.J., Healy, E., Luger, T.A., Schwarz, T., and Schwarz, A. (2005). alpha-Melanocyte-stimulating hormone protects from ultraviolet radiation-induced apoptosis and DNA damage. J Biol Chem *280*, 5795-5802.

Bouvier, D., Hubert, J., Seve, A.P., and Bouteille, M. (1985). Characterization of lamina-bound chromatin in the nuclear shell isolated from HeLa cells. Exp Cell Res *156*, 500-512.

Bustin, M., Catez, F., and Lim, J.H. (2005). The dynamics of histone H1 function in chromatin. Mol Cell *17*, 617-620.

Cadet, J., Douki, T., Ravanat, J.L., and Di Mascio, P. (2009). Sensitized formation of oxidatively generated damage to cellular DNA by UVA radiation. Photochem Photobiol Sci *8*, 903-911.

Cann, K.L., and Dellaire, G. (2011). Heterochromatin and the DNA damage response: the need to relax. Biochem Cell Biol *89*, 45-60.

Carrier, F., Georgel, P.T., Pourquier, P., Blake, M., Kontny, H.U., Antinore, M.J., Gariboldi, M., Myers, T.G., Weinstein, J.N., Pommier, Y*., et al.* (1999). Gadd45, a p53-responsive stress protein, modifies DNA accessibility on damaged chromatin. Mol Cell Biol *19*, 1673-1685.

Carruthers, L.M., and Hansen, J.C. (2000). The core histone N termini function independently of linker histones during chromatin condensation. J Biol Chem *275*, 37285-37290.

Chakravarthy, S., Park, Y.J., Chodaparambil, J., Edayathumangalam, R.S., and Luger, K. (2005). Structure and dynamic properties of nucleosome core particles. FEBS letters *579*, 895-898.

Chathoth, S., Thayyullathil, F., Hago, A., Shahin, A., Patel, M., and Galadari, S. (2009). UVC-induced apoptosis in Dubca cells is independent of JNK activation and p53(Ser-15) phosphorylation. Biochem Biophys Res Commun *383*, 426-432.

Ciccia, A., and Elledge, S.J. (2010). The DNA damage response: making it safe to play with knives. Mol Cell *40*, 179-204.

Crompton, M., Virji, S., and Ward, J.M. (1998). Cyclophilin-D binds strongly to complexes of the voltage-dependent anion channel and the adenine nucleotide translocase to form the permeability transition pore. Eur J Biochem *258*, 729-735.

Dahle, J., and Kvam, E. (2003). Induction of delayed mutations and chromosomal instability in fibroblasts after UVA-, UVB-, and X-radiation. Cancer Res *63*, 1464-1469.

Danial, N.N., and Korsmeyer, S.J. (2004). Cell death: critical control points. Cell *116*, 205-219.

Dechat, T., Adam, S.A., and Goldman, R.D. (2009). Nuclear lamins and chromatin: when structure meets function. Adv Enzyme Regul *49*, 157-166.

Decraene, D., Agostinis, P., Pupe, A., de Haes, P., and Garmyn, M. (2001). Acute response of human skin to solar radiation: regulation and function of the p53 protein. Journal of photochemistry and photobiology B, Biology *63*, 78-83.

Dillon, N. (2008). The impact of gene location in the nucleus on transcriptional regulation. Dev Cell *15*, 182-186.

Dinant, C., Bartek, J., and Bekker-Jensen, S. (2012). Histone displacement during nucleotide excision repair. Int J Mol Sci *13*, 13322-13337.

Dinant, C., Houtsmuller, A.B., and Vermeulen, W. (2008). Chromatin structure and DNA damage repair. Epigenetics Chromatin *1*, 9.

Douki, T. (2006). Low ionic strength reduces cytosine photoreactivity in UVC-irradiated isolated DNA. Photochemical & photobiological sciences : Official journal of the European Photochemistry Association and the European Society for Photobiology *5*, 1045-1051.

Douki, T. (2013). The variety of UV-induced pyrimidine dimeric photoproducts in DNA as shown by chromatographic quantification methods. Photochem Photobiol Sci *12*, 1286-1302.

Douki, T., Bretonniere, Y., and Cadet, J. (2000). Protection against radiation-induced degradation of DNA bases by polyamines. Radiat Res *153*, 29-35.

Downing, K.H. (2000). Structural basis for the interaction of tubulin with proteins and drugs that affect microtubule dynamics. Annu Rev Cell Dev Biol *16*, 89-111.

Farkas, E., Ujvarosi, K., Nagy, G., Posta, J., and Banfalvi, G. (2010). Apoptogenic and necrogenic effects of mercuric acetate on the chromatin structure of K562 human erythroleukemia cells. Toxicol In Vitro *24*, 267-275.

Finch, J.T., and Klug, A. (1976). Solenoidal model for superstructure in chromatin. Proc Natl Acad Sci U S A *73*, 1897-1901.

Fraser, P., and Bickmore, W. (2007). Nuclear organization of the genome and the potential for gene regulation. Nature *447*, 413-417.

Friedberg, E.C. (2003). DNA damage and repair. Nature *421*, 436-440.

Friedberg, E.C., Aguilera, A., Gellert, M., Hanawalt, P.C., Hays, J.B., Lehmann, A.R., Lindahl, T., Lowndes, N., Sarasin, A., and Wood, R.D. (2006). DNA repair: from molecular mechanism to human disease. DNA Repair (Amst) *5*, 986-996.

Fullgrabe, J., Hajji, N., and Joseph, B. (2010). Cracking the death code: apoptosis-related histone modifications. Cell Death Differ *17*, 1238-1243.

Fuss, J.O., and Tainer, J.A. (2011). XPB and XPD helicases in TFIIH orchestrate DNA duplex opening and damage verification to coordinate repair with transcription and cell cycle via CAK kinase. DNA repair *10*, 697-713.

Gan, H.H., and Schlick, T. (2010). Chromatin ionic atmosphere analyzed by a mesoscale electrostatic approach. Biophys J *99*, 2587-2596.

Goodsell, D.S. (2001). The molecular perspective: ultraviolet light and pyrimidine dimers. Oncologist *6*, 298-299.

Gospodinov, A., and Herceg, Z. (2013). Shaping chromatin for repair. Mutat Res *752*, 45-60.

Gray-Schopfer, V., Wellbrock, C., and Marais, R. (2007). Melanoma biology and new targeted therapy. Nature *445*, 851-857.

Green, C.M., and Almouzni, G. (2002). When repair meets chromatin. First in series on chromatin dynamics. EMBO Rep *3*, 28-33.

Green, D.R., and Kroemer, G. (2004). The pathophysiology of mitochondrial cell death. Science *305*, 626-629.

Grigoryev, S.A., Arya, G., Correll, S., Woodcock, C.L., and Schlick, T. (2009). Evidence for heteromorphic chromatin fibers from analysis of nucleosome interactions. Proc Natl Acad Sci U S A *106*, 13317-13322.

Groisman, R., Polanowska, J., Kuraoka, I., Sawada, J., Saijo, M., Drapkin, R., Kisselev, A.F., Tanaka, K., and Nakatani, Y. (2003). The ubiquitin ligase activity in the DDB2 and CSA complexes is differentially regulated by the COP9 signalosome in response to DNA damage. Cell *113*, 357-367.

Gross-Bellard, M., Oudet, P., and Chambon, P. (1973). Isolation of high-molecular-weight DNA from mammalian cells. Eur J Biochem *36*, 32-38.

Hamilton, C., Hayward, R.L., and Gilbert, N. (2011). Global chromatin fibre compaction in response to DNA damage. Biochem Biophys Res Commun *414*, 820-825.

Hansen, J.C. (2002). Conformational dynamics of the chromatin fiber in solution: determinants, mechanisms, and functions. Annu Rev Biophys Biomol Struct *31*, 361-392.

He, H., and Lehming, N. (2003). Global effects of histone modifications. Briefings in functional genomics & proteomics *2*, 234-243.

He, Y.J., McCall, C.M., Hu, J., Zeng, Y., and Xiong, Y. (2006). DDB1 functions as a linker to recruit receptor WD40 proteins to CUL4-ROC1 ubiquitin ligases. Genes Dev *20*, 2949-2954.

Hendzel, M.J., Lever, M.A., Crawford, E., and Th'ng, J.P. (2004). The C-terminal domain is the primary determinant of histone H1 binding to chromatin in vivo. J Biol Chem *279*, 20028-20034.

Henning, K.A., Li, L., Iyer, N., McDaniel, L.D., Reagan, M.S., Legerski, R., Schultz, R.A., Stefanini, M., Lehmann, A.R., Mayne, L.V.*, et al.* (1995). The Cockayne syndrome group A gene encodes a WD repeat protein that interacts with CSB protein and a subunit of RNA polymerase II TFIIH. Cell *82*, 555-564.

Hergeth, S.P., and Schneider, R. (2015). The H1 linker histones: multifunctional proteins beyond the nucleosomal core particle. EMBO Rep *16*, 1439-1453.

Herrling, T., Jung, K., and Fuchs, J. (2006). Measurements of UV-generated free radicals/reactive oxygen species (ROS) in skin. Spectrochim Acta A Mol Biomol Spectrosc *63*, 840-845.

Hihara, S., Pack, C.G., Kaizu, K., Tani, T., Hanafusa, T., Nozaki, T., Takemoto, S., Yoshimi, T., Yokota, H., Imamoto, N.*, et al.* (2012). Local nucleosome dynamics facilitate chromatin accessibility in living mammalian cells. Cell Rep *2*, 1645-1656.

Hochberg, M., Kohen, R., and Enk, C.D. (2006). Role of antioxidants in prevention of pyrimidine dimer formation in UVB irradiated human HaCaT keratinocytes. Biomed Pharmacother *60*, 233-237.

Horn, P.J., and Peterson, C.L. (2002). Molecular biology. Chromatin higher order folding--wrapping up transcription. Science *297*, 1824-1827.

Huen, M.S., and Chen, J. (2010). Assembly of checkpoint and repair machineries at DNA damage sites. Trends Biochem Sci *35*, 101-108.

Hunt, C.R., Ramnarain, D., Horikoshi, N., Iyengar, P., Pandita, R.K., Shay, J.W., and Pandita, T.K. (2013). Histone modifications and DNA double-strand break repair after exposure to ionizing radiations. Radiat Res *179*, 383-392.

Ichihashi, M., Ueda, M., Budiyanto, A., Bito, T., Oka, M., Fukunaga, M., Tsuru, K., and Horikawa, T. (2003). UV-induced skin damage. Toxicology *189*, 21-39.

Igney, F.H., and Krammer, P.H. (2002). Death and anti-death: tumour resistance to apoptosis. Nat Rev Cancer *2*, 277-288.

Imai, S., Johnson, F.B., Marciniak, R.A., McVey, M., Park, P.U., and Guarente, L. (2000). Sir2: an NAD-dependent histone deacetylase that connects chromatin silencing, metabolism, and aging. Cold Spring Harb Symp Quant Biol *65*, 297-302.

Jordan, M.A., and Wilson, L. (1998). Microtubules and actin filaments: dynamic targets for cancer chemotherapy. Curr Opin Cell Biol *10*, 123-130.

Jurkiewicz, B.A., and Buettner, G.R. (1994). Ultraviolet light-induced free radical formation in skin: an electron paramagnetic resonance study. Photochem Photobiol *59*, 1-4.

Kahl, C.R., and Means, A.R. (2003). Regulation of cell cycle progression by calcium/calmodulin-dependent pathways. Endocr Rev *24*, 719-736.

Kalverda, B., Roling, M.D., and Fornerod, M. (2008). Chromatin organization in relation to the nuclear periphery. FEBS Lett *582*, 2017-2022.

Kornberg, R.D., and Lorch, Y. (1999a). Chromatin-modifying and -remodeling complexes. Curr Opin Genet Dev *9*, 148-151.

Kornberg, R.D., and Lorch, Y. (1999b). Twenty-five years of the nucleosome, fundamental particle of the eukaryote chromosome. Cell *98*, 285-294.

Kornberg, R.D., and Thomas, J.O. (1974). Chromatin structure; oligomers of the histones. Science *184*, 865-868.

Korolev, N., Allahverdi, A., Yang, Y., Fan, Y., Lyubartsev, A.P., and Nordenskiold, L. (2010). Electrostatic origin of salt-induced nucleosome array compaction. Biophys J *99*, 1896-1905.

Korolev, N., Zhao, Y., Allahverdi, A., Eom, K.D., Tam, J.P., and Nordenskiold, L. (2012). The effect of salt on oligocation-induced chromatin condensation. Biochem Biophys Res Commun *418*, 205-210.

Kulms, D., and Schwarz, T. (2000). Molecular mechanisms of UV-induced apoptosis. Photodermatol Photoimmunol Photomed *16*, 195-201.

Lachner, M., O'Carroll, D., Rea, S., Mechtler, K., and Jenuwein, T. (2001). Methylation of histone H3 lysine 9 creates a binding site for HP1 proteins. Nature *410*, 116-120.

Lane, J.D., Allan, V.J., and Woodman, P.G. (2005). Active relocation of chromatin and endoplasmic reticulum into blebs in late apoptotic cells. J Cell Sci *118*, 4059-4071.

Lange, S.S., Mitchell, D.L., and Vasquez, K.M. (2008). High mobility group protein B1 enhances DNA repair and chromatin modification after DNA damage. Proc Natl Acad Sci U S A *105*, 10320-10325.

Lin, J., Chen, F., Sun, M.J., Zhu, J., Li, Y.W., Pan, L.Z., Zhang, J., and Tan, J.H. (2016). The relationship between apoptosis, chromatin configuration, histone modification and competence of oocytes: A study using the mouse ovary-holding stress model. Sci Rep *6*, 28347.

Lin, Y., and Wilson, J.H. (2007). Transcription-induced CAG repeat contraction in human cells is mediated in part by transcription-coupled nucleotide excision repair. Molecular and cellular biology *27*, 6209-6217.

Lomberk, G., Wallrath, L., and Urrutia, R. (2006). The Heterochromatin Protein 1 family. Genome Biol *7*, 228.

Loyola, A., and Almouzni, G. (2007). Marking histone H3 variants: how, when and why? Trends in biochemical sciences *32*, 425-433.

Luger, K., Mader, A.W., Richmond, R.K., Sargent, D.F., and Richmond, T.J. (1997). Crystal structure of the nucleosome core particle at 2.8 A resolution. Nature *389*, 251-260.

Luijsterburg, M.S., and van Attikum, H. (2011). Chromatin and the DNA damage response: the cancer connection. Mol Oncol *5*, 349-367.

Maeshima, K., Rogge, R., Tamura, S., Joti, Y., Hikima, T., Szerlong, H., Krause, C., Herman, J., Seidel, E., DeLuca, J.*, et al.* (2016). Nucleosomal arrays self-assemble into supramolecular globular structures lacking 30-nm fibers. EMBO J *35*, 1115-1132.

Mateos-Langerak, J., Goetze, S., Leonhardt, H., Cremer, T., van Driel, R., and Lanctot, C. (2007). Nuclear architecture: Is it important for genome function and can we prove it? J Cell Biochem *102*, 1067-1075.

Mattout-Drubezki, A., and Gruenbaum, Y. (2003). Dynamic interactions of nuclear lamina proteins with chromatin and transcriptional machinery. Cell Mol Life Sci *60*, 2053-2063.

Misteli, T. (2007). Beyond the sequence: cellular organization of genome function. Cell *128*, 787-800.

Miyamura, Y., Coelho, S.G., Wolber, R., Miller, S.A., Wakamatsu, K., Zmudzka, B.Z., Ito, S., Smuda, C., Passeron, T., Choi, W.*, et al.* (2007). Regulation of human skin pigmentation and responses to ultraviolet radiation. Pigment Cell Res *20*, 2-13.

Moan, J., Nielsen, K.P., and Juzeniene, A. (2012). Immediate pigment darkening: its evolutionary roles may include protection against folate photosensitization. FASEB J *26*, 971-975.

Neves-Costa, A., and Varga-Weisz, P. (2006). The roles of chromatin remodelling factors in replication. Results and problems in cell differentiation *41*, 91-107.

Nielsen, A.L., Oulad-Abdelghani, M., Ortiz, J.A., Remboutsika, E., Chambon, P., and Losson, R. (2001). Heterochromatin formation in mammalian cells: interaction between histones and HP1 proteins. Mol Cell *7*, 729-739.

Norwood, L.E., Grade, S.K., Cryderman, D.E., Hines, K.A., Furiasse, N., Toro, R., Li, Y., Dhasarathy, A., Kladde, M.P., Hendrix, M.J.*, et al.* (2004). Conserved properties of HP1(Hsalpha). Gene *336*, 37-46.

Ogi, T., Limsirichaikul, S., Overmeer, R.M., Volker, M., Takenaka, K., Cloney, R., Nakazawa, Y., Niimi, A., Miki, Y., Jaspers, N.G.*, et al.* (2010). Three DNA polymerases, recruited by different mechanisms, carry out NER repair synthesis in human cells. Molecular cell *37*, 714-727.

Oksenych, V., and Coin, F. (2010). The long unwinding road: XPB and XPD helicases in damaged DNA opening. Cell cycle *9*, 90-96.

Palomera-Sanchez, Z., and Zurita, M. (2011). Open, repair and close again: chromatin dynamics and the response to UV-induced DNA damage. DNA repair *10*, 119-125.

Park, S.B., Huh, C.H., Choe, Y.B., and Youn, J.I. (2002). Time course of ultraviolet-induced skin reactions evaluated by two different reflectance spectrophotometers: DermaSpectrophotometer and Minolta spectrophotometer CM-2002. Photodermatol Photoimmunol Photomed *18*, 23-28.

Passarge, E. (1979). Emil Heitz and the concept of heterochromatin: longitudinal chromosome differentiation was recognized fifty years ago. American journal of human genetics *31*, 106-115.

Pecinka, A., and Mittelsten Scheid, O. (2012). Stress-induced chromatin changes: a critical view on their heritability. Plant Cell Physiol *53*, 801-808.

Peterson, C.L., and Laniel, M.A. (2004). Histones and histone modifications. Curr Biol *14*, R546-551.

Pfeifer, G.P. (1997). Formation and processing of UV photoproducts: effects of DNA sequence and chromatin environment. Photochem Photobiol *65*, 270-283.

Pillai, S., Oresajo, C., and Hayward, J. (2005). Ultraviolet radiation and skin aging: roles of reactive oxygen species, inflammation and protease activation, and strategies for prevention of inflammation-induced matrix degradation - a review. Int J Cosmet Sci *27*, 17-34.

Pincelli, C., and Marconi, A. (2010). Keratinocyte stem cells: friends and foes. J Cell Physiol *225*, 310-315.

Polo, S.E., and Almouzni, G. (2015). Chromatin dynamics after DNA damage: The legacy of the access-repair-restore model. DNA Repair (Amst) *36*, 114-121.

Pruitt, S.C., and Grainger, R.M. (1980). A repeating unit of higher order chromatin structure in chick red blood cell nuclei. Chromosoma *78*, 257-274.

Rando, O.J., and Winston, F. (2012). Chromatin and transcription in yeast. Genetics *190*, 351-387.

Ransom, M., Dennehey, B.K., and Tyler, J.K. (2010). Chaperoning histones during DNA replication and repair. Cell *140*, 183-195.

Rastogi, R.P., Richa, Kumar, A., Tyagi, M.B., and Sinha, R.P. (2010). Molecular mechanisms of ultraviolet radiation-induced DNA damage and repair. J Nucleic Acids *2010*, 592980.

Robinson, P.J., Fairall, L., Huynh, V.A., and Rhodes, D. (2006). EM measurements define the dimensions of the "30-nm" chromatin fiber: evidence for a compact, interdigitated structure. Proc Natl Acad Sci U S A *103*, 6506-6511.

Robinson, P.J., and Rhodes, D. (2006). Structure of the '30 nm' chromatin fibre: a key role for the linker histone. Curr Opin Struct Biol *16*, 336-343.

Roots, R., and Okada, S. (1975). Estimation of life times and diffusion distances of radicals involved in x-ray-induced DNA strand breaks of killing of mammalian cells. Radiat Res *64*, 306-320.

Roque, A., Iloro, I., Ponte, I., Arrondo, J.L., and Suau, P. (2005). DNA-induced secondary structure of the carboxyl-terminal domain of histone H1. J Biol Chem *280*, 32141-32147.

Roque, A., Ponte, I., and Suau, P. (2016). Interplay between histone H1 structure and function. Biochim Biophys Acta *1859*, 444-454.

Ruan, K., Yamamoto, T.G., Asakawa, H., Chikashige, Y., Kimura, H., Masukata, H., Haraguchi, T., and Hiraoka, Y. (2015). Histone H4 acetylation required for chromatin decompaction during DNA replication. Sci Rep *5*, 12720.

Sage, E. (1993). Distribution and repair of photolesions in DNA: genetic consequences and the role of sequence context. Photochem Photobiol *57*, 163-174.

Schirmer, E.C., and Foisner, R. (2007). Proteins that associate with lamins: many faces, many functions. Exp Cell Res *313*, 2167-2179.

Schlick, T., Hayes, J., and Grigoryev, S. (2012). Toward convergence of experimental studies and theoretical modeling of the chromatin fiber. J Biol Chem *287*, 5183-5191.

Schmitges, F.W., Prusty, A.B., Faty, M., Stutzer, A., Lingaraju, G.M., Aiwazian, J., Sack, R., Hess, D., Li, L., Zhou, S.*, et al.* (2011). Histone methylation by PRC2 is inhibited by active chromatin marks. Mol Cell *42*, 330-341.

Schneider, R., and Grosschedl, R. (2007). Dynamics and interplay of nuclear architecture, genome organization, and gene expression. Genes Dev *21*, 3027-3043.

Schwarz, A., Stander, S., Berneburg, M., Bohm, M., Kulms, D., van Steeg, H., Grosse-Heitmeyer, K., Krutmann, J., and Schwarz, T. (2002). Interleukin-12 suppresses ultraviolet radiation-induced apoptosis by inducing DNA repair. Nat Cell Biol *4*, 26-31.

Scrima, A., Konickova, R., Czyzewski, B.K., Kawasaki, Y., Jeffrey, P.D., Groisman, R., Nakatani, Y., Iwai, S., Pavletich, N.P., and Thoma, N.H. (2008). Structural basis of UV DNA-damage recognition by the DDB1-DDB2 complex. Cell *135*, 1213-1223.

Shogren-Knaak, M., Ishii, H., Sun, J.M., Pazin, M.J., Davie, J.R., and Peterson, C.L. (2006). Histone H4-K16 acetylation controls chromatin structure and protein interactions. Science *311*, 844-847.

Skelding, K.A., Rostas, J.A., and Verrills, N.M. (2011). Controlling the cell cycle: the role of calcium/calmodulin-stimulated protein kinases I and II. Cell Cycle *10*, 631-639.

Slominski, A., and Pawelek, J. (1998). Animals under the sun: effects of ultraviolet radiation on mammalian skin. Clin Dermatol *16*, 503-515.

Smerdon, M.J. (1991). DNA repair and the role of chromatin structure. Curr Opin Cell Biol *3*, 422-428.

Smerdon, M.J., Tlsty, T.D., and Lieberman, M.W. (1978). Distribution of ultraviolet-induced DNA repair synthesis in nuclease sensitive and resistant regions of human chromatin. Biochemistry *17*, 2377-2386.

Smith, K.T., and Workman, J.L. (2012). Chromatin proteins: key responders to stress. PLoS biology *10*, e1001371.

Soria, G., Polo, S.E., and Almouzni, G. (2012). Prime, repair, restore: the active role of chromatin in the DNA damage response. Mol Cell *46*, 722-734.

Soutoglou, E., and Misteli, T. (2008). Activation of the cellular DNA damage response in the absence of DNA lesions. Science *320*, 1507-1510.

Spotheim-Maurizot, M., Ruiz, S., Sabattier, R., and Charlier, M. (1995). Radioprotection of DNA by polyamines. Int J Radiat Biol *68*, 571-577.

Strayer, D.S., Hoek, J.B., Thomas, A.P., and White, M.K. (1999). Cellular activation by Ca2+ release from stores in the endoplasmic reticulum but not by increased free Ca2+ in the cytosol. Biochem J *344 Pt 1*, 39-46.

Strick, R., Strissel, P.L., Gavrilov, K., and Levi-Setti, R. (2001). Cation-chromatin binding as shown by ion microscopy is essential for the structural integrity of chromosomes. J Cell Biol *155*, 899-910.

Suzuki, K., Yamauchi, M., Oka, Y., Suzuki, M., and Yamashita, S. (2010). A novel and simple micro-irradiation technique for creating localized DNA double-strand breaks. Nucleic Acids Res *38*, e129.

Takata, H., Hanafusa, T., Mori, T., Shimura, M., Iida, Y., Ishikawa, K., Yoshikawa, K., Yoshikawa, Y., and Maeshima, K. (2013). Chromatin compaction protects genomic DNA from radiation damage. PLoS One *8*, e75622.

Takata, H., Uchiyama, S., Nakamura, N., Nakashima, S., Kobayashi, S., Sone, T., Kimura, S., Lahmers, S., Granzier, H., Labeit, S.*, et al.* (2007). A comparative proteome analysis of human metaphase chromosomes isolated from two different cell lines reveals a set of conserved chromosome-associated proteins. Genes Cells *12*, 269-284.

Tan, R., and Lan, L. (2016). Guarding chromosomes from oxidative DNA damage to the very end. Acta Biochim Biophys Sin (Shanghai) *48*, 617-622.

Tjeertes, J.V., Miller, K.M., and Jackson, S.P. (2009). Screen for DNA-damage-responsive histone modifications identifies H3K9Ac and H3K56Ac in human cells. EMBO J *28*, 1878-1889.

Tombes, R.M., and Borisy, G.G. (1989). Intracellular free calcium and mitosis in mammalian cells: anaphase onset is calcium modulated, but is not triggered by a brief transient. J Cell Biol *109*, 627-636.

Trinkle-Mulcahy, L., and Lamond, A.I. (2008). Nuclear functions in space and time: gene expression in a dynamic, constrained environment. FEBS Lett *582*, 1960-1970.

Trojer, P., and Reinberg, D. (2007). Facultative heterochromatin: is there a distinctive molecular signature? Molecular cell *28*, 1-13.

Tumbar, T., Sudlow, G., and Belmont, A.S. (1999). Large-scale chromatin unfolding and remodeling induced by VP16 acidic activation domain. J Cell Biol *145*, 1341-1354.

Vanhaecke, T., Papeleu, P., Elaut, G., and Rogiers, V. (2004). Trichostatin A-like hydroxamate histone deacetylase inhibitors as therapeutic agents: toxicological point of view. Curr Med Chem *11*, 1629-1643.

Visvanathan, A., Ahmed, K., Even-Faitelson, L., Lleres, D., Bazett-Jones, D.P., and Lamond, A.I. (2013). Modulation of Higher Order Chromatin Conformation in Mammalian Cell Nuclei Can Be Mediated by Polyamines and Divalent Cations. PLoS One *8*, e67689.

Volker, M., Mone, M.J., Karmakar, P., van Hoffen, A., Schul, W., Vermeulen, W., Hoeijmakers, J.H., van Driel, R., van Zeeland, A.A., and Mullenders, L.H. (2001). Sequential assembly of the nucleotide excision repair factors in vivo. Molecular cell *8*, 213-224.

Wang, S.H., Nan, R., Accardo, M.C., Sentmanat, M., Dimitri, P., and Elgin, S.C. (2014). A distinct type of heterochromatin at the telomeric region of the Drosophila melanogaster Y chromosome. PLoS One *9*, e86451.

Warters, R.L., Newton, G.L., Olive, P.L., and Fahey, R.C. (1999). Radioprotection of human cell nuclear DNA by polyamines: radiosensitivity of chromatin is influenced by tightly bound spermine. Radiat Res *151*, 354-362.

Wasmeier, C., Hume, A.N., Bolasco, G., and Seabra, M.C. (2008). Melanosomes at a glance. J Cell Sci *121*, 3995-3999.

Wicks, N.L., Chan, J.W., Najera, J.A., Ciriello, J.M., and Oancea, E. (2011). UVA phototransduction drives early melanin synthesis in human melanocytes. Curr Biol *21*, 1906-1911.

Widom, J. (1986). Physicochemical studies of the folding of the 100 A nucleosome filament into the 300 A filament. Cation dependence. J Mol Biol *190*, 411-424.

Wong, R.S. (2011). Apoptosis in cancer: from pathogenesis to treatment. J Exp Clin Cancer Res *30*, 87.

Woodcock, C.L. (2006). Chromatin architecture. Curr Opin Struct Biol *16*, 213-220.

Woodcock, C.L., Frado, L.L., and Rattner, J.B. (1984). The higher-order structure of chromatin: evidence for a helical ribbon arrangement. J Cell Biol *99*, 42-52.

Woodcock, C.L., and Ghosh, R.P. (2010). Chromatin higher-order structure and dynamics. Cold Spring Harb Perspect Biol *2*, a000596.

Woodcock, C.L., Skoultchi, A.I., and Fan, Y. (2006). Role of linker histone in chromatin structure and function: H1 stoichiometry and nucleosome repeat length. Chromosome Res *14*, 17-25.

Yang, J.C., and Cortopassi, G.A. (1998). Induction of the mitochondrial permeability transition causes release of the apoptogenic factor cytochrome c. Free Radic Biol Med *24*, 624-631.

Yu, Y., Teng, Y., Liu, H., Reed, S.H., and Waters, R. (2005). UV irradiation stimulates histone acetylation and chromatin remodeling at a repressed yeast locus. Proc Natl Acad Sci U S A *102*, 8650-8655.

Zeng, W., Ball, A.R., Jr., and Yokomori, K. (2010). HP1: heterochromatin binding proteins working the genome. Epigenetics *5*, 287-292.

Ziv, Y., Bielopolski, D., Galanty, Y., Lukas, C., Taya, Y., Schultz, D.C., Lukas, J., Bekker-Jensen, S., Bartek, J., and Shiloh, Y. (2006). Chromatin relaxation in response to DNA double-strand breaks is modulated by a novel ATM- and KAP-1 dependent pathway. Nat Cell Biol *8*, 870-876.